FINAL REPORT

PART II

The Study of Space Communications Spread Spectrum Systems

REPORT 88-2

PREPARED FOR THE DEPARTMENT OF COMMUNICATIONS
UNDER DSS CONTRACT NO. 36001-6-3530/0/ST

IC
Department of Electrical Engineering
Queen's University at Kingston
Kingston, Ontario, Canada

FINAL REPORT

PART II

The Study of Space Communications Spread Spectrum Systems

REPORT 88-2

PREPARED FOR THE DEPARTMENT OF COMMUNICATIONS
UNDER DSS CONTRACT NO. 36001-6-3530/0/ST

SECURITY CLASSIFICATION OF FORM
(highest classification of Title, Abstract, Keywords)

DOCUMENT CONTROL DATA

(Security classification of title, body of abstract and indexing annotation must be entered when the overall document is classified)

1. ORIGINATOR (the name and address of the organization preparing the document. Organizations for whom the document was prepared, e.g. Establishment sponsoring a contractor's report, or tasking agency, are entered in section B.)

Department of Electrical Engineering,
QUEEN'S UNIVERSITY,
KINGSTON, Ontario, Canada. K7L 3N6

2. SECURITY CLASSIFICATION (overall security classification of the document. including special warning terms if applicable)

Unclassified.

3. TITLE (the complete document title as indicated on the title page. Its classification should be indicated by the appropriate abbreviation (S,C,R or U) in parentheses after the title.)

"The Study of Space Communications Spread Spectrum Systems"
Part II - Trellis Coding for Noncoherent Frequency-Hopped Communications Systems

4. AUTHORS (Last name, first name, middle initial. If military, show rank, e.g. Doe, Maj. John E.)

Wearring, M.G., Wittke, P.H.

5. DATE OF PUBLICATION (month and year of publication of document)

March, 1988

6a. NO. OF PAGES (total containing information. Include Annexes, Appendices, etc.)

82

6b. NO. OF REFS (total cited in document)

22

7. DESCRIPTIVE NOTES (the category of the document, e.g. technical report, technical note or memorandum. If appropriate, enter the type of report, e.g. interim, progress, summary, annual or final. Give the inclusive dates when a specific reporting period is covered.)

Final Report Part II

8. SPONSORING ACTIVITY (the name of the department project office or laboratory sponsoring the research and development. Include the address.)

Communications Research Centre, Department of Communications, 3701 Carling Avenue,
P.O. Box 11490, Station 'H', OTTAWA, Ontario. K2H 8S2

9a. PROJECT OR GRANT NO. (If appropriate, the applicable research and development project or grant number under which the document was written. Please specify whether project or grant)

32A99

9b. CONTRACT NO. (if appropriate, the applicable number under which the document was written)

DSS Contract 36001-6-3530/0/ST

10a. ORIGINATOR'S DOCUMENT NUMBER (the official document number by which the document is identified by the originating activity. This number must be unique to this document.)

Report 88-2, Department of Electrical Engineering, Queen's Univ., Kingston, Ont.

10b. OTHER DOCUMENT NOS. (Any other numbers which may be assigned this document either by the originator or by the sponsor)

11. DOCUMENT AVAILABILITY (any limitations on further dissemination of the document, other than those imposed by security classification)

(x) Unlimited distribution
( ) Distribution limited to defence departments and defence contractors; further distribution only as approved
( ) Distribution limited to defence departments and Canadian defence contractors; further distribution only as approved
( ) Distribution limited to government departments and agencies; further distribution only as approved
( ) Distribution limited to defence departments; further distribution only as approved
( ) Other (please specify):

12. DOCUMENT ANNOUNCEMENT (any limitation to the bibliographic announcement of this document. This will normally correspond to the Document Availabilty (11). However, where further distribution (beyond the audience specified in 11) is possible, a wider announcement audience may be selected.)

No Limitation.

Unclassified

SECURITY CLASSIFICATION OF FORM

DCD03 9/04/87

13. ABSTRACT (a brief and factual summary of the document. It may also appear elsewhere in the body of the document itself. It is highly desirable that the abstract of classified documents be unclassified. Each paragraph of the abstract shall begin with an indication of the security classification of the information in the paragraph (unless the document itself is unclassified) represented as (S), (C), (R), or (U). It is not necessary to include here abstracts in both official languages unless the text is bilingual).

In noncoherent frequency hopped spread spectrum communication systems, M-ary frequency shift keying (FSK) is the usual form of modulation. In this paper, coded systems are studied which consist of convolutional codes with the codewords mapped onto multiple tone signal sets. The signals employ the same set of orthogonal tones as M-ary FSK, but several tones may be transmitted simultaneously. This allows an increase in the number of signals, to accommodate the redundant information introduced by the coding, without any bandwidth expansion. Some of Ungerboeck's rules for assigning signals to the trellis branches are employed.

The results were obtained for transmission over an additive white Gaussian noise channel with both coherent and noncoherent detection. Viterbi decoding was used, with both hard and soft decoding metrics. Simulation results and error bounds are presented. Seven different coded modulations which encompass information rates of 1, 2, and 3 bits per signalling interval, and employ sets of 2, 3, 4, or 8 orthogonal tones, are considered. Of the codes provided, the minimum performance improvement is 2 dB compared to the reference M-ary FSK. The maximum improvement achieved was 4.6 dB for the case of two tones. As would be expected, the best performance is obtained with soft decision decoding.

14. KEYWORDS, DESCRIPTORS or IDENTIFIERS (technically meaningful terms or short phrases that characterize a document and could be helpful in cataloguing the document. They should be selected so that no security classification is required. Identifiers, such as equipment model designation, trade name, military project code name, geographic location may also be included. If possible, keywords should be selected from a published thesaurus. e.g. Thesaurus of Engineering and Scientific Terms (TEST) and that thesaurus identified. If it is not possible to select indexing terms which are Unclassified, the classification of each should be indicated as with the title.)

Frequency hopped spread spectrum systems, coding, trellis coding, non coherent reception.

TRELLIS CODING FOR NONCOHERENT FREQUENCY-HOPPED COMMUNICATIONS SYSTEMS

by

M. G. Wearring

P. H. Wittke

REPORT 88-5

FINAL REPORT PART II

(OF IV PARTS)

PREPARED FOR THE DEPARTMENT OF COMMUNICATIONS

UNDER DSS CONTRACT NO. 36001-6-3530/0/ST

"The Study of Space Communications Spread Spectrum Systems"

Department of Electrical Engineering

Queen's University

Kingston, Ontario, Canada

March, 1988

ABSTRACT

In noncoherent frequency hopped spread spectrum communication systems, M-ary frequency shift keying (FSK) is the usual form of modulation. In this paper, coded systems are studied which consist of convolutional codes with the codewords mapped onto multiple tone signal sets. The signals employ the same set of orthogonal tones as M-ary FSK, but several tones may be transmitted simultaneously. This allows an increase in the number of signals, to accommodate the redundant information introduced by the coding, without any bandwidth expansion. Some of Ungerboeck's rules for assigning signals to the trellis branches are employed.

The results were obtained for transmission over an additive white Gaussian noise channel with both coherent and noncoherent detection. Viterbi decoding was used, with both hard and soft decoding metrics. Simulation results and error bounds are presented. Seven different coded modulations which encompass information rates of 1, 2, and 3 bits per signalling interval, and employ sets of 2, 3, 4, or 8 orthogonal tones, are considered. Of the codes provided, the minimum performance improvement is 2 dB compared to the reference M-ary FSK. The maximum improvement achieved was 4.6 dB for the case of two tones. As would be expected, the best performance is obtained with soft decision decoding.

TABLE OF CONTENTS

LIST OF FIGURES

LIST OF TABLES

CHAPTER ONE

INTRODUCTION

1.1 Background

The purpose of this study is to investigate methods of improving the performance of a communications system by the use of coding. A block diagram of the coded system under consideration appears in Figure 1.1. The actual system is intended for digital satellite communications, and may be incorporated into a frequency hopped spread spectrum anti-jam application. The type of modulation considered is frequency shift keying (FSK) in which one of several different tones is sent in each signalling interval. Details of the modulation scheme and the receivers employed are given in Chapter two.

The basic principle of coding is that redundant information is added to the information bit stream so that transmission errors may be detected and/or corrected. Because of this redundant information, more signals must be sent over the channel to maintain the same information transfer rate as in the uncoded case. This can be accomplished by using the same set of signals at a faster signalling rate, or by increasing the number of signals used (signal set expansion). Both of these methods usually require a larger bandwidth than the original uncoded scheme for noncoherent FSK signalling. Alternatively, the information rate may be lowered to maintain the same bandwidth occupancy.

The goal of this study is to find a method of improving the system performance without sacrificing the data rate or increasing the bandwidth required. In frequency

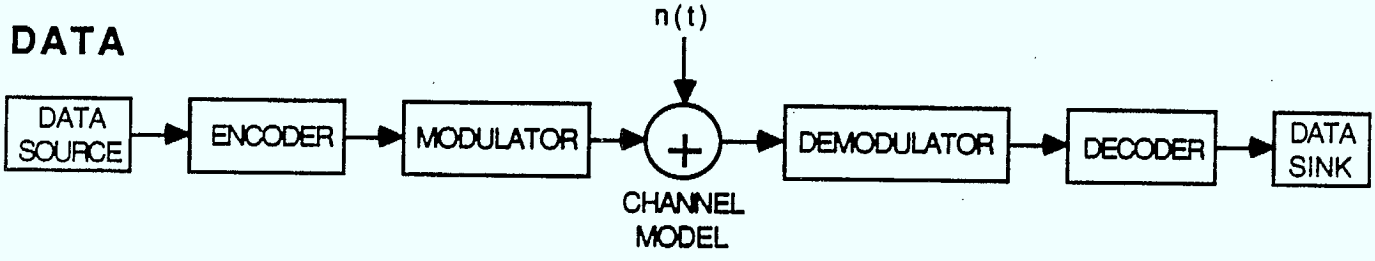

Figure 1.1 System Block Diagram

hopped systems, the processing gain is the ratio of the overall system bandwidth to the bandwidth occupied during each hop, and it indicates the ability of the system to reject jamming noise. Increasing the modulation bandwidth decreases the processing gain of the system, which is undesirable. The technique proposed in this study is to use convolutional codes with Viterbi decoding to improve error performance. The signal set is expanded by the use of multiple tone signals to accommodate the redundant bits, instead of the single tones which are used in conventional M-ary FSK. This does not increase the modulation bandwidth and thereby affect the processing gain. This study considers the performance of the encoder/decoder and modulator/receiver over an additive white Gaussian noise (AWGN) channel.

1.2 Literature Review

There have been several studies of the application of conventional coding to noncoherent anti-jam communication systems [1,2,3,4]. These papers explore the use of various codes to reduce the effect of a partial band jamming signal. Block codes, convolutional codes, and repetition codes (diversity) have all been investigated, as well as different combinations of concatenated codes. Reed-Solomon codes and convolutional codes both have good performance, especially when combined with diversity. Conventional M-ary FSK modulation was employed in all cases, and usually bandwidth expansion was allowed to accommodate the coding. Both hard and soft decision demodulation have been considered. Hard decision receivers select which signal is closest to the transmitted signal and relay that decision to the decoder. A metric, which is proportional to the logarithm of the probability that each signal was received, is computed by a soft decision receiver and used by the decoder. In a jamming environment, soft decision decoding is not desirable unless there is side information

about the presence of the jammer, because jammed signals seriously degrade the operation of the decoder. If side information is available, soft decision demodulation gives the best performance; otherwise hard decisions are superior [1]. This report does not consider the effects of jamming or frequency hopping on the communication system, but considers the performance in white noise. It is noteworthy that convolutional codes showed good performance under jamming conditions [3,4]. The Viterbi decoder is also readily adaptable to accept hard or soft demodulator decision variables.

There are two papers which consider the application of coding to noncoherent FSK signalling [5,6]. They both employ conventional M-ary modulation schemes and require bandwidth expansion or reduced data rate to accommodate the coding. The first study [5] considers continuous phase FSK, which has phase continuity between tones in subsequent signalling intervals, and also uses non-orthogonal tone spacings. The demodulation technique, although noncoherent, makes use of the phase continuity and employs an unconventional receiver structure. Practical frequency hopped systems, where the hopping occurs over large bandwidths, cannot maintain phase continuity between hops, and so these modulations are inappropriate. Keightley [6] studied the use of convolutional codes with binary and 4-ary FSK. Noncoherent demodulation with hard decisions was used for application to a frequency hopped spread spectrum system. The coding gain observed at a bit error rate (BER) of 10^{-5} was approximately 2 dB in the binary case, and negligible in the 4-ary case. The codes employed had rates of 1/2 and 1/3 with constraint lengths of 7 and 8 respectively. Thus the system transmission rates were reduced to 1/2 and 1/3.

Much work has been done recently on trellis coding [7,8,9,10] and a functioning system has been implemented in a modem. This technique provides large coding gains

without bandwidth expansion or reduction of data rate. All of the documented studies have been confined to coherent communication systems, in which the carrier may be both amplitude and/or phase modulated. The uncoded signal set is expanded by adding different levels of phase and amplitude modulation without requiring additional bandwidth. The resulting expanded signal constellation contains a symmetrical array of signal points. This signal set is partitioned or subdivided into subsets which have increasing distances between signal points in the subsets. The signal points are then assigned to the codewords of a convolutional code, according to a set of rules designed to provide maximum coding gain. This study employs some of the concepts of trellis coding applied to FSK signal sets. The signal constellations are expanded by using multiple tone signals so that additional bandwidth is not required. Signal set partitioning is also carried out, but not in the same manner as in coherent systems. The multiple tone signal constellations cannot be partitioned into subsets with increasing spacing between signal points. However, some of the rules from trellis coding are employed when mapping codewords onto signals. It is anticipated that the application of the principles of trellis coding will provide significant coding gains because of the success realized in coherent systems.

1.3 Report Summary

This report is divided into four chapters. An indication of the problem under consideration and the extent of research in this area has been given in the introductory chapter. Chapter two contains a detailed theoretical explanation of the various components in the system. First the modulation scheme and the structure of the different receivers is explained, followed by a description of the error correcting codes and the operation of the decoder. The second chapter concludes with an explanation of how the

coding and modulation schemes are combined in the overall system and presents some bounds on error performance. There are seven different cases which were investigated, and their characteristics are detailed in this chapter.

In general, the problem of theoretically evaluating the error performance of the noncoherent coded system does not appear tractable, and so computer simulations were carried out. Chapter three is a presentation of the results of the simulation programs. A brief description of the program structure is given first, followed by error performance curves for each of the seven cases considered. The results for all the cases are summarized in a table and then the performance of each case is discussed in detail.

Chapter four contains the general conclusions which may be derived from the simulation results. Suggestions for further research on this problem are given also.

CHAPTER TWO

THEORY

2.1 Modulation

2.1.1 Modulation Scheme

The reference modulation for this study is M-ary FSK. This scheme is commonly used in frequency hopped spread spectrum satellite systems for digital communication [1,6]. One of a set of M tones is sent in each signalling interval (T seconds). The number of tones (M) may be 2, 4, 8, or 16 corresponding to 1, 2, 3, or 4 bits of information per signal. The tones are orthogonally spaced in the frequency domain, which entails a minimum frequency difference of 1/2T hertz between adjacent tones.

The alternative modulation schemes, which allow coding without rate reduction, are divided into two types. The first expanded modulation technique employs the same set of orthogonal tones, but more than one tone can be transmitted in each interval (jT,(j+1)T). All possible combinations of the M tones are used, and the signal space is expanded to 2^M signals which transmit M bits per symbol period. This multiple tone signal constellation does not require any additional bandwidth, but there are other considerations. The transmitter requires increased power to send several tones simultaneously, if each tone has the same energy as a single tone in the reference system. The different modulation schemes will be compared with the same **average** signal energy, but the variation in energy between signals for this multiple tone case

could require a transmitter with a larger peak power capability. This signal constellation also includes a zero signal (no tones sent), which could be undesirable in some systems.

The spacing of signals in the constellation has a significant effect on the system performance. In the reference M-ary FSK system, the single orthogonal tones are equidistant in the signal space. The multiple tone signals with constant energy tones form the vertices of a hypercube in M dimensional space, where M is the number of tones. This can best be visualized in three dimensions as shown in Figure 2.1. This first type of modulation is used in four of the seven cases to be considered. Case 1A employs two tones, Case 2A employs three tones, and both Cases 2B and 3A use four tone signal sets.

The second type of multiple tone signal set was devised to reduce the variation in signal amplitude among the various possible signals. The same set of orthogonal tones is again employed. Instead of permitting all possible tone combinations, a more limited subset is allowed to comprise the signal set. For the two and four tone cases, only single tones and pairs of tones are used as signals. The eight tone case employs single tones and sets of three tones. The pairs and triples of tones have the amplitude of each tone reduced so that the signal energy is equal to that of a single tone signal. The zero signal is excluded from these signal sets and therefore the signal energy is constant for this scheme. This makes demodulation simpler as will be explained in the discussion of receiver structure.

The constant signal energy multiple tone scheme is used in three cases which were simulated. Case 1B employs two tones and thus only three signals are available in each signal interval. These signals are $s_1(t) = \cos \omega_1 t$, $s_2(t) = \cos \omega_2 t$, and $s_3(t) = (\cos \omega_1 t + \cos \omega_2 t)/ \sqrt{2}$. The modulation is performed over two symbol intervals

(a) Single Tone (FSK)

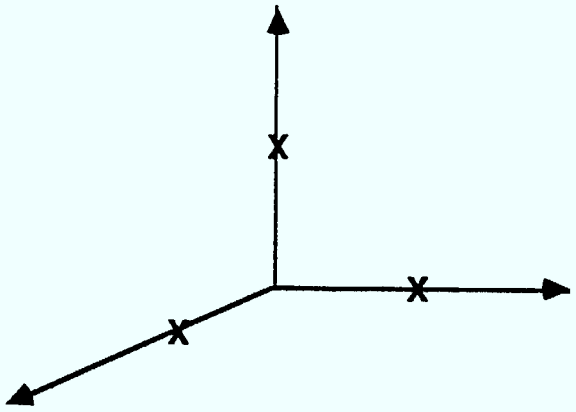

(b) Multiple Tone (constant energy tones)

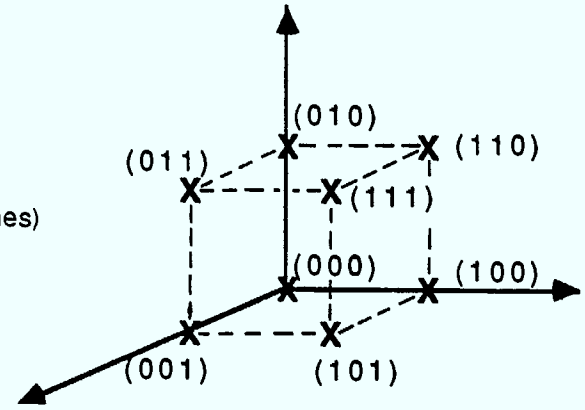

(c) Multiple Tone (constant signal energy)

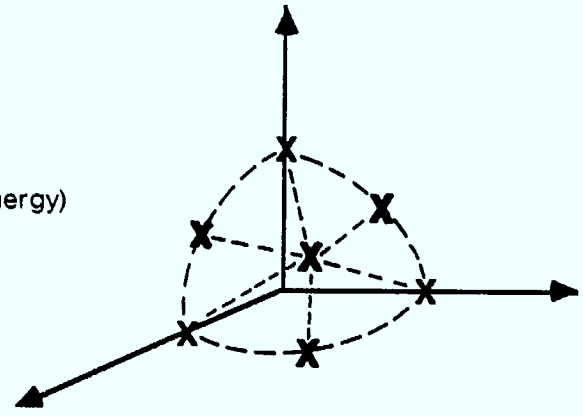

Figure 2.1 Signal Constellations

(2T) so that nine possible combinations, using three signals per period, are available. Eight of these points were chosen to represent three bits of data in each interval of 2T. For the case of four tones, there are four single tone signals and six different possible pairs of tones. Simulation Case 2C employs eight of these ten signals in the constellation. This allows three bits to be transmitted during each symbol interval (T seconds). The final case employing the second alternative modulation scheme is designated number 3B and uses eight orthogonal tones. There are eight signals containing a single tone and fifty-six possible three tone combinations. The combined signal constellation has sixty-four signal points which permits transmission of six binary digits with each signal.

The multiple tone modulations with constant signal energy have an irregular spacing between points in the signal constellation. The maximum spacing between signals is the same as the distance between orthogonal tones, and occurs between signals with no tones in common. When signals possess common tones, the spacing is reduced. The more tones in common between two signals, the smaller the distance between the two. The amplitudes of the tones in common between the signals also affect the spacing. This irregular spacing must be considered when mapping code words onto the signal points, and is discussed in the third section of this chapter.

2.1.2 Coherent Receiver

The coherent receiver is the optimum receiver for reception in the presence of additive white Gaussian noise (AWGN) when the phase of the transmitted signal is known. Then the local oscillator is perfectly matched to the incoming tones to eliminate any phase offset. This receiver cannot be used in the frequency hopped spread

spectrum system because phase continuity between subsequent signal tones and between frequency hops is not provided by practical transmitters. These phase jumps, and the phase offsets introduced during transmission, preclude the matching of the local oscillator to the transmitted signal. However, the coherent receiver provides the best possible performance that could be achieved, and will be included for purposes of comparison. The structure of the coherent receiver is simpler than the noncoherent receiver, and this allows a simulation to be performed more quickly and easily. Also, the performance of the coherent receiver can be readily analyzed, and there are theoretical results that provide verification of the simulation program. If coherent demodulation was actually used, a more efficient modulation scheme than FSK would likely be employed.

The usual optimum coherent receiver [11, p. 235; 12, p. 49] calculates the squared Euclidean distance between the received signal (r(t)), and each of the possible transmitted signals ($s_i(t)$). A decision is made in favour of the signal closest to the received signal, based on the minimum of the computed distances. The squared distance is given by

$$\begin{aligned} d_i^2 &= \int_0^T [r(t) - s_i(t)]^2 dt \\ &= \int_0^T r^2(t)dt - 2\int_0^T r(t)s_i(t)dt + \int_0^T s_i^2(t)dt \end{aligned} \tag{2.1}$$

The first term in (2.1) is constant, independent of the index i, and so may be neglected in the search for the nearest $s_i(t)$. The remaining two terms can be multiplied by -1/2 to form a decision variable which is now maximized.

$$L_i = \int_0^T r(t)s_i(t)dt - \frac{1}{2}\int_0^T s_i^2(t)dt$$
$$= q_i - \frac{1}{2}E_i \qquad (2.2)$$

The structure of this receiver is well-known [11, p. 235; 12, p. 49] and is shown for two cases in Figure 2.2. The receiver for conventional binary FSK is shown in part (a) of the diagram, where $s_1(t) = \cos \omega_1 t$ and $s_2(t) = \cos \omega_2 t$. The multiple tone scheme with different signal energies is demodulated by the system in part (b). In this case, the signals are $s_0(t) = 0$, $s_1(t) = \cos \omega_1 t$, $s_2(t) = \cos \omega_2 t$, and $s_3(t) = \cos \omega_1 t + \cos \omega_2 t$. For constant energy signals, E_i is constant for all i, and the decision variable becomes simply q_i . The decision variables for multiple tone signals are in general obtained by summing the variables for each tone in the signal, and scaling to account for the signal energy. This means that the multiple tone receiver requires only one correlator for each tone.

The theoretical error probabilities for uncoded signalling are easily obtained for the baseline system of M-ary FSK with coherent reception. The probability of symbol error for an orthogonal signal set over an AWGN channel is given by [11, p. 257; 13, p. 120]

$$P_S = 1 - \int_{-\infty}^{\infty} p_n(\alpha - \sqrt{E_S})d\alpha \left[\int_{-\infty}^{\alpha} p_n(\beta)d\beta \right]^{M-1} \qquad (2.3)$$

where M is the number of signals (ie. tones) and

$$p_n(\alpha) = \frac{1}{\sqrt{2\pi}} \exp \frac{-\alpha^2}{2}$$

is the Gaussian probability density function. The bit error probability is obtained from the symbol error probability as

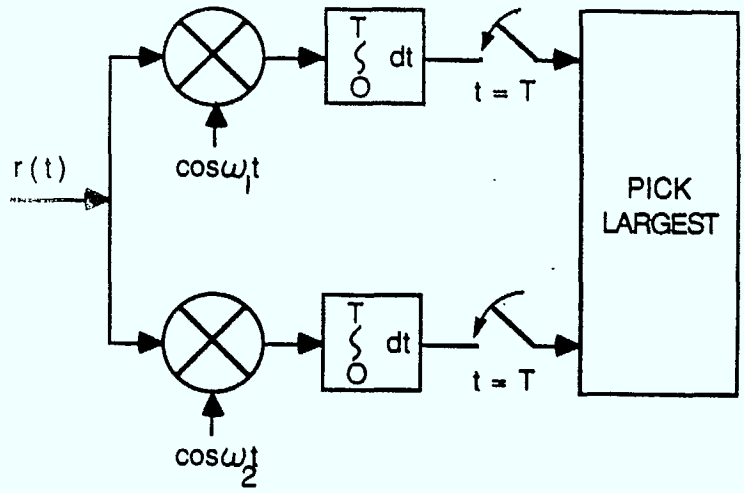

(a) Single Tone Binary FSK

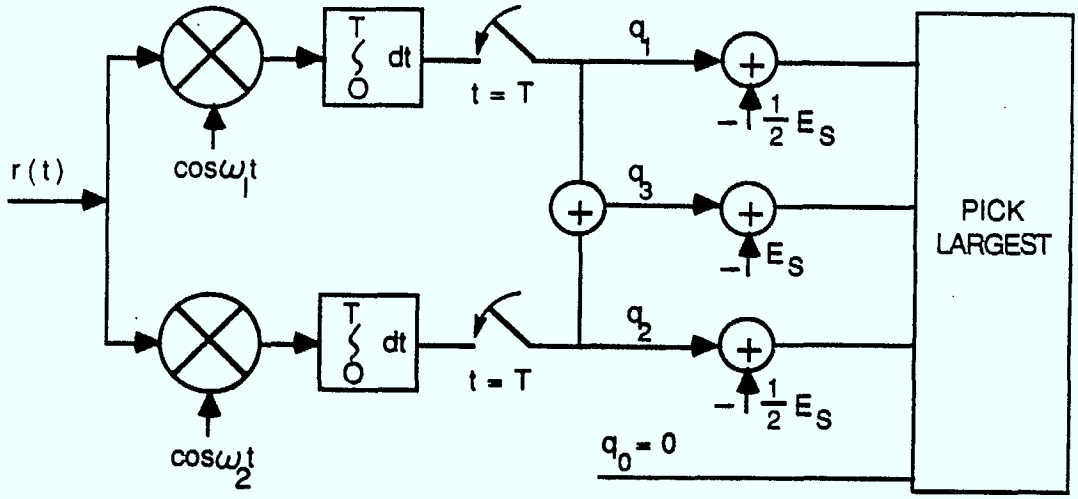

(b) Multiple Tone FSK (2 tones)

Figure 2.2 Coherent Receiver

$$P_B = \frac{\frac{1}{2}M}{M-1}P_S \tag{2.4}$$

The integral in equation (2.3) is tabulated in Golomb [13, p. 196] and these results were used for the baseline performance curves with coherent reception.

The theoretical performance may also be obtained for the case of multiple tone signalling with constant energy **tones.** With the ideal coherent receiver, the signal constellation may be considered as a rectangular signal set [11, p. 254] with error probabilities given by

$$P_S = 1 - (1-p)^M \tag{2.5}$$

$$P_B = p = Q\left(\frac{d}{\sqrt{2N_0}}\right) \tag{2.6}$$

where

M is the number of dimensions (ie. the number of tones),

$$Q(x) = \int_x^\infty \frac{1}{\sqrt{2\pi}} \exp -\frac{t^2}{2} dt$$

$$d = \sqrt{E_S}$$

E_S is the energy of a single tone, and

N_0 is the spectral density of the Gaussian noise in watts/hertz.

The multiple tone signalling schemes with constant signal energy do not form a rectangular signal set. Because of the irregular spacing of the signals, the probability of error varies with the signal that was sent, due to the different proximities of other signals. This does not allow for a simple expression for the error performance as in the previous cases, and the results are obtained strictly by simulation.

2.1.3 Noncoherent Receiver

The introduction of a random phase angle (θ) into the received signal, increases the complexity required for the optimum receiver. The structure of this noncoherent receiver is common [11, p. 519; 12, p. 104], and is shown in Figure 2.3. Two receivers appear in the diagram. Case (a) demodulates conventional binary FSK, where $s_1(t) = \cos \omega_1 t$ and $s_2(t) = \cos \omega_2 t$. In part (b), multiple tone signals with all possible combinations of two tones, and variable signal energy are demodulated. The signals for this receiver are $s_0(t) = 0$, $s_1(t) = \cos \omega_1 t$, $s_2(t) = \cos \omega_2 t$, and $s_3(t) = \cos \omega_1 t + \cos \omega_2 t$. There are two correlators for each signal, one in phase and one in quadrature, whose outputs are combined to negate the effect of the random phase. Multiple tone signals are assumed to have the same phase angle for all tones, and the probability distribution of the random phase is considered to be uniformly distributed between 0 and 2π radians.

This receiver calculates the probability of the received signal, given that the ith signal was sent, for all members i of the signal set. This probability is known as the likelihood function, and its logarithm is used as the decision variable. The signal with the maximum probability is chosen as the transmitted signal. The development of the theory for this receiver is rather lengthy, and can be found in the references [11, p. 511; 12, p.103], and so just the decision variable itself will be given here as

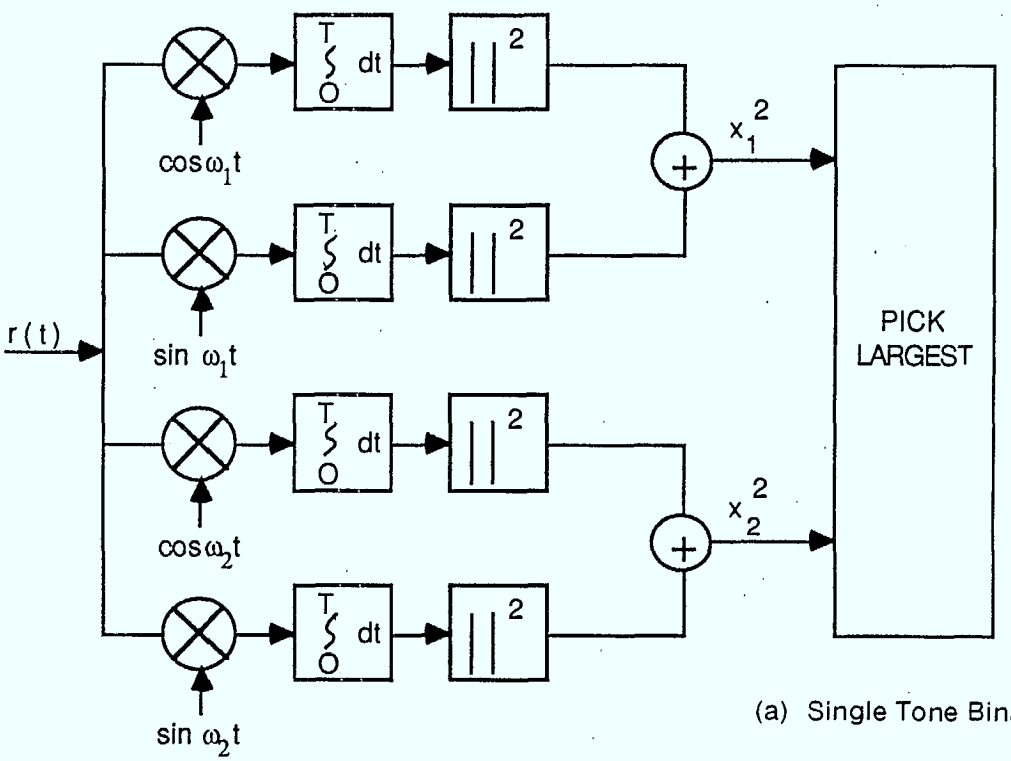

(a) Single Tone Binary FSK

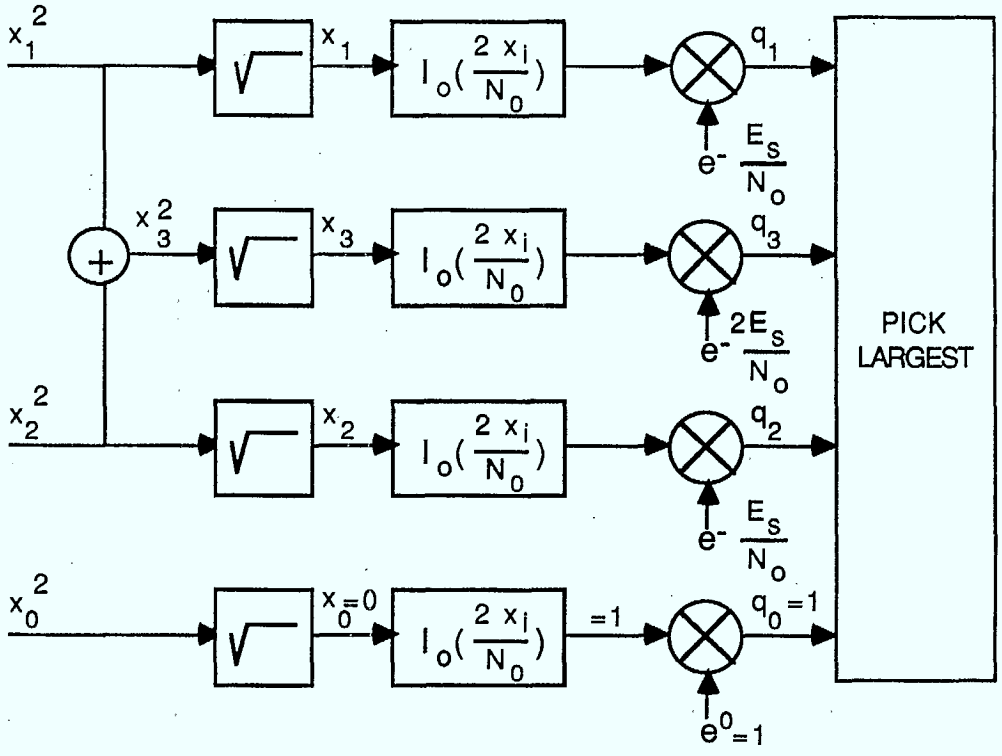

(b) Multiple Tone FSK (2 tones)

Figure 2.3 Noncoherent Receiver

$$L_i = \ln\left[I_0\left(\frac{2X_i}{N_0}\right) \exp\left(-\frac{E_i}{N_0}\right)\right] \tag{2.7}$$

where

$$I_0(x) = \frac{1}{2\pi}\int_0^{2\pi} \exp[x\cos(\theta + \alpha)]d\theta$$

is the zero order modified Bessel function of the first kind,

$$E_i = \int_0^T s_i^2(t)dt$$

is the energy of the ith signal,

N_0 is the spectral density of the Gaussian noise in watts/hertz, and

$$X_i^2 = \left[\int_0^T r(t)s_i(t)dt\right]^2 + \left[\int_0^T r(t)\hat{s}_i(t)dt\right]^2 \tag{2.8}$$

is the sum of the squares of the correlator outputs for the in-phase and quadrature components of the correlation with the ith signal.

$s_i(t)$ is the in phase component of the signal since the signals are made up of cosine tones, and

$\hat{s}_i(t)$ is the quadrature component of the signal, which consists of sine tones at the same frequencies.

As was the case for the coherent receiver, the decision variables for multiple tone signals can be obtained from the correlator outputs for the individual tones. This means that only one pair of correlators is required for each tone in the system. The signal $s_i(t)$ giving rise to the maximum L_i is chosen as the signal sent.

For the baseline system and other constant signal energy cases, the decision variables can be further simplified. The exponential function in (2.7) will be a constant because E_i is the same for each index i, and so it can be ignored. To maximize the modified Bessel function, it is only necessary to maximize its argument because the Bessel function is a monotone increasing function. Therefore the optimum decision will be made by maximizing X_i or X_i^2. This receiver simplification results in the structure shown in Figure 2.3 (a), and is also known as square-law combining. The multiple tone modulation system with unequal signal energies cannot employ the simplified decision variables obtained from the correlator outputs. The modified Bessel function and the exponential function must be calculated in order to make a maximum likelihood decision.

The theoretical symbol error probability for noncoherent M-ary FSK is given by [11, p. 577]

$$P_S = \sum_{k=1}^{M-1} \frac{(-1)^{k+1}}{k+1} \binom{M-1}{k} \exp\left(-\frac{k}{k+1}\frac{E_S}{N_0}\right) \tag{2.9}$$

where

$$\binom{A}{B} = \frac{A!}{B!(A-B)!}$$

and the bit error probability is

$$P_B = \frac{\frac{1}{2}M}{M-1}P_S \tag{2.10}$$

The theoretical performance of the multiple tone noncoherent receiver is difficult to obtain. The presence of the Bessel function and the exponential function in the decision variables of the variable signal energy case makes the analysis difficult. The constant signal energy multiple tone modulation has irregular signal spacings which impedes the evaluation of theoretical error probabilities.

2.2 Coding

2.2.1 Description of Codes

Convolutional encoding with Viterbi decoding is one of the more widely used methods of forward error correction. This is due to the ease of implementation and the relatively large coding gains obtainable from simple codes. As previously mentioned, this coding technique was chosen for consideration in this report. There are several different ways to describe convolutional codes, which will be briefly summarized below. More information on convolutional codes may be obtained from the references [12, p. 227; 14, p.227].

The first way to visualize a convolutional encoder is as a binary shift register with taps connected to modulo two adders. The information bit stream is shifted into the register in groups of b bits, and there are n modulo two adders which produce n output bits for each codeword. The rate of a code is given by the ratio b/n, which is the ratio

of input to output bits. The number of b-tuples in the shift register is denoted by k, and so the encoder retains b(k - 1) bits of the previous input data which define the state of the encoder. The value $\nu = b(k - 1)$ is defined as the constraint length of the code, and is the logarithm to the base two of the number of states. The length of the shift register (bk) is sometimes considered as the constraint length, but the previous definition (ν) will be used here as it is more useful for comparing codes of different rates. As the b-tuples of input data are shifted into the register, the state of the encoder changes and the output data is determined by the tap connections from the register to the adders. These connections are usually specified by generator polynomials or a generator matrix. A simple code with rate 1/2 and constraint length 2 is used as an example throughout this section. A diagram showing the shift register tap connections and the generator matrix appears in Figure 2.4.

Another way to describe a convolutional code is by means of a trellis diagram. The states of the code are assigned to nodes in the trellis and branches between states indicate a particular input and corresponding output symbol. It is obvious that a given input data sequence can be mapped onto a certain path through the trellis. There are 2^b branches which emerge from each node, corresponding to each of the possible inputs. The branches remerge at the next stage in the trellis in groups of 2^b at each state. The trellis for the example code is shown in Figure 2.5.

The final representation of a convolutional code is by a state diagram. The states of the code are again assigned to nodes in the diagram, and directed paths between states correspond to particular input and output symbols. The state diagram can be used to obtain the generating function of a code, which allows the weight profile to be determined. The state diagram for the model code appears in Figure 2.6.

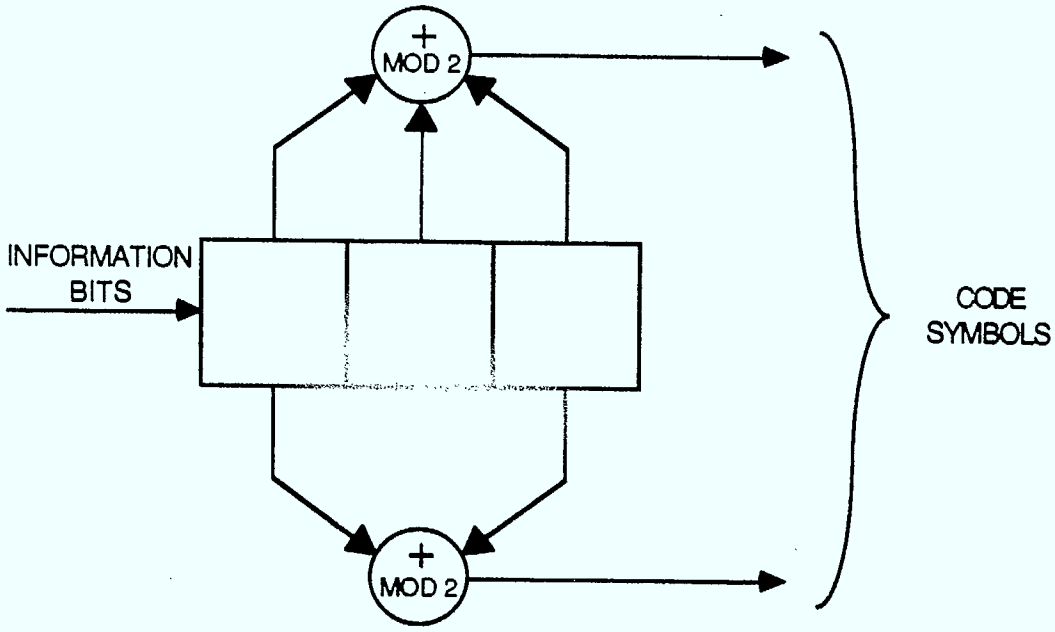

$G = [\ 11\ \ 01\ \ 11\ ]$

$\nu = 2$

$k = 3$

Figure 2.4 Convolutional Encoder

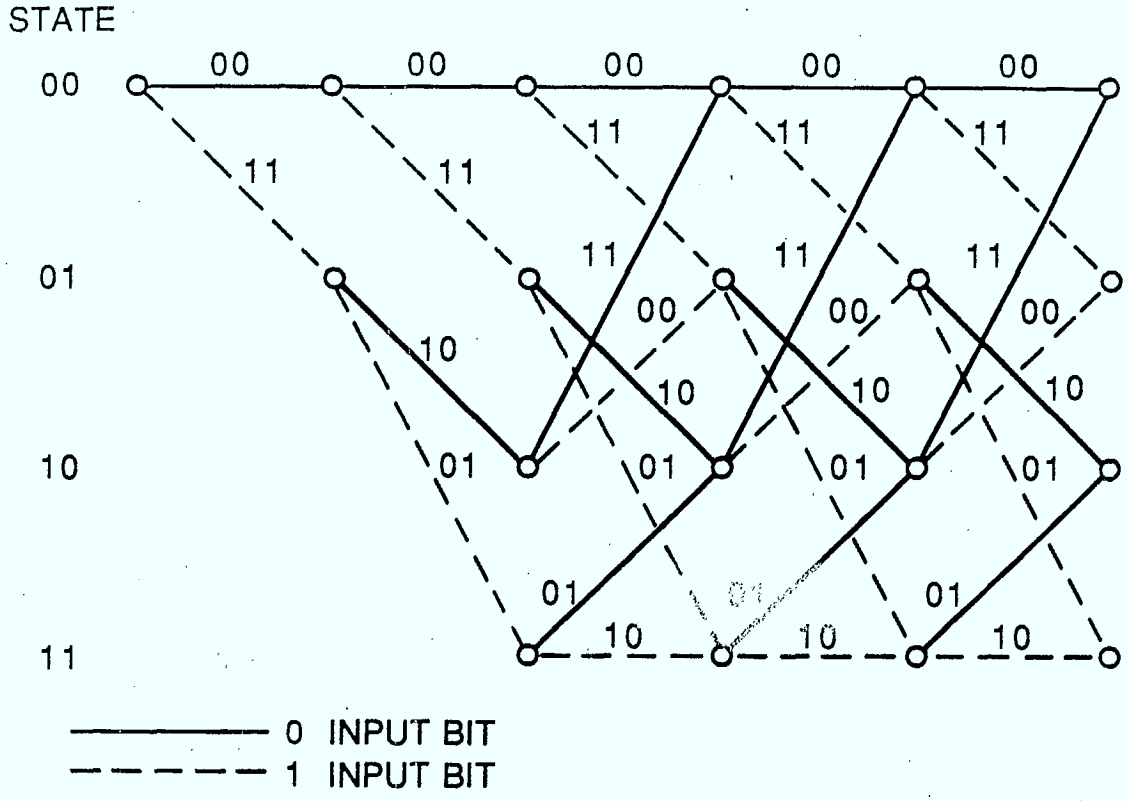

Figure 2.5 Trellis Diagram

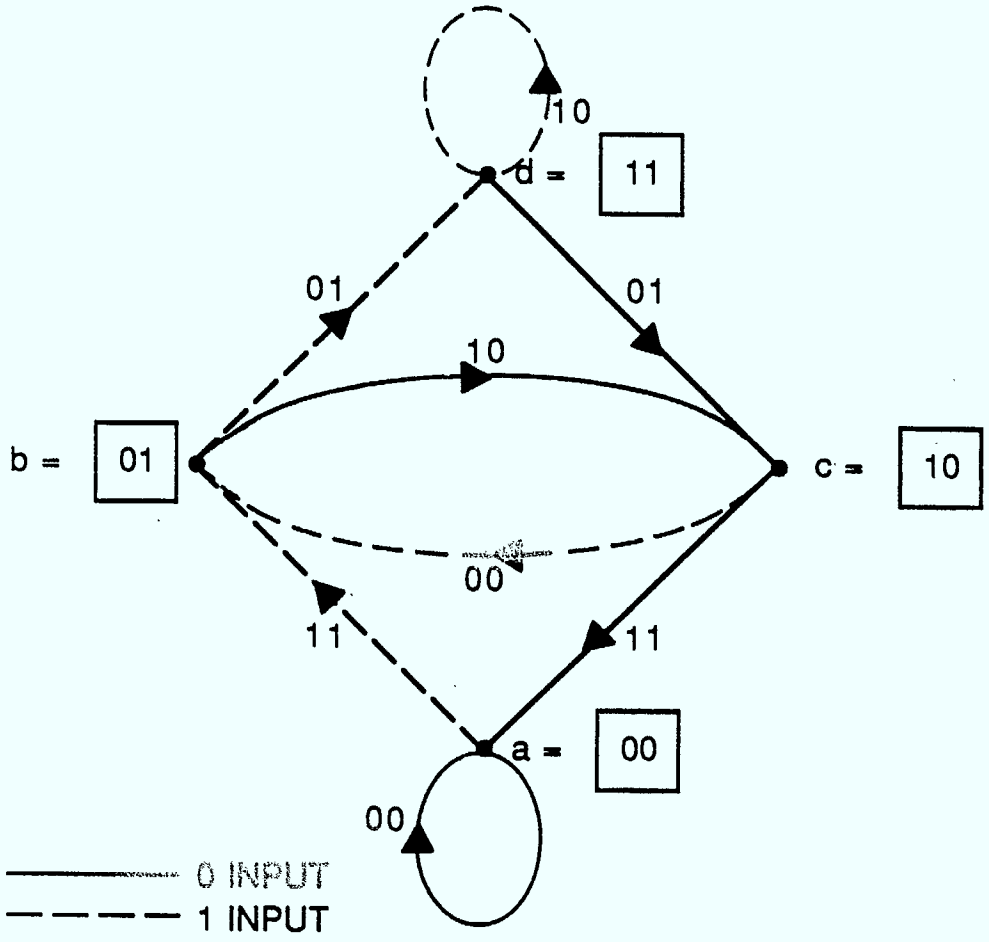

Figure 2.6 State Diagram

The weight profile is significant because it directly affects the error performance of the code. All the codes under consideration are linear, and therefore the all zeroes path may be considered as the correct path for the purpose of analysis. The weight or distance profile is obtained from the set of paths which diverge from the correct path and then remerge, corresponding to possible error events. The distance measure, for hard decision decoding, is the Hamming distance between the error path and the correct path. This is the number of output bits in which the two paths differ. These paths may be observed in the trellis diagram, and the weight profile obtained by adding up the Hamming weight of the output symbols along all paths which diverge from and then remerge with the all zeroes path.

A more tractable description of the weight profile is the code generating function. If the state diagram is redrawn with the zero state split, all the paths originating in one half of the zero state, passing through the other states, and entering the other half of the zero state will represent error paths. The branches of the state diagram are labelled

$$D^a L I^b \tag{2.11}$$

where

D represents the distance or output weight,

L represents the length of the path,

I represents the input weight,

a is the Hamming weight of the output symbol, and

b is the Hamming weight of the input symbol.

Using signal flow graph theory, the state equations of the diagram are solved to yield the generating function T(D,L,I). This function has the form of an infinite sum of products of D, L, and I. The coefficient of each term represents the number of paths with distance of the exponent of D, input weight of the exponent of I, and length of the exponent of L. The sum may also be represented as a fraction of polynomials in D, L, and I. To obtain the weight profile, L and I are made equal to unity. The resulting function T(D) yields the number of paths at various distances from the correct path. The redrawn state diagram and the code generating function of the example code are shown in Figure 2.7. The free distance (d_f) is the minimum distance of any error path from the correct path, and is a good indicator of how well the code will perform.

The codes used in this study were obtained from other papers which investigated optimal codes [15, 16, 17]. The best codes had maximum free distance (d_f) for given code rate and constraint length. Only relatively short constraint length codes were used so that Viterbi decoding could be utilized. The optimal rate 1/2 codes were used in Case 1A [15]. They were also combined to form a rate 2/4 code for Case 2B and a rate 3/6 code for Case 3B. A dual-3 rate 1/2 code was also considered in Case 3B [17]. Rate 2/3 codes with maximum d_f were employed in Cases 1B, 2A, and 2C while rate 3/4 codes comprised Case 3A [16]. The various code generator matrices are shown in Table 2.1 and a complete description of each case appears in Table 3.1.

2.2.2 Maximum Likelihood Decoding

There has been much published work on the decoding of convolutional codes [12, p. 235; 18, 19, 20]. The Viterbi algorithm for maximum likelihood sequence estimation is

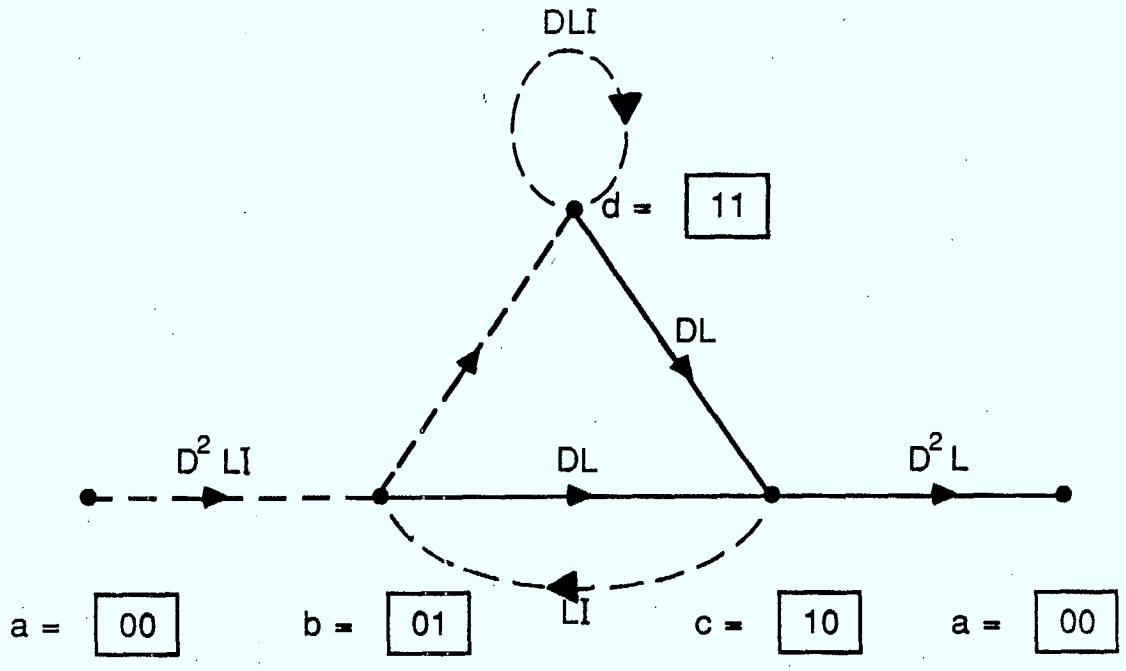

$$T(D,L,I) = \frac{D^5L^3I}{1 - DL(1+L)I}$$
$$= D^5L^3I + D^6L^4(1+L)I^2 + \cdots + D^{5+k}L^{3+k}(1+L)^kI^{1+k} + \cdots$$

$$T(D) = \frac{D^5}{1-2D}$$
$$= D^5 + 2D^6 + \cdots + 2^kD^{k+5} + \cdots$$

Figure 2.7 Generating Function

TABLE 2.1

Convolutional Code Generator Matrices

Rate	Constraint Length	Free Distance	Generator Matrix
1/2	2	5	[11 01 11]
1/2	6	10	[11 01 11 11 00 10 11]
2/3	4	5	$\begin{bmatrix} 101\ 100\ 110 \\ 011\ 101\ 011 \end{bmatrix}$
2/3	6	7	$\begin{bmatrix} 101\ 111\ 010\ 101 \\ 011\ 111\ 101\ 011 \end{bmatrix}$
2/4	6	6	$\begin{bmatrix} 1100\ 1100\ 0100\ 1100 \\ 0011\ 0011\ 0001\ 0011 \end{bmatrix}$
3/4	5	5	$\begin{bmatrix} 1001\ 1111\ 0000 \\ 0101\ 0101\ 1001 \\ 0011\ 0100\ 0011 \end{bmatrix}$
3/6	3	6	$\begin{bmatrix} 100100\ 100101 \\ 010010\ 010100 \\ 001001\ 001010 \end{bmatrix}$
3/6	6	5	$\begin{bmatrix} 110000\ 010000\ 110000 \\ 001100\ 000100\ 001100 \\ 000011\ 000001\ 000011 \end{bmatrix}$

the most popular decoding technique for codes of short constraint length. This technique was investigated as being the most likely to be employed for a digital satellite channel. A brief summary of the decoding operation follows.

The basic problem can be most easily visualized as selecting the best path through the code trellis, based on information from the receiver. The maximum a posteriori probability for the path is used as the selection criterion. A decision metric for each branch is computed based on the received signal in each signalling interval. The metric is proportional to the logarithm of the likelihood function, in keeping with the coding literature [12, p. 238; 21, p. 188]. This metric is maximized by the decoder. The metric may also be considered as a distance measure between code vectors, in which case the negative log likelihood would be used and the decoder would perform minimization of the metric. Proceeding with the convention adopted, we have

$$p(\mathbf{r} \mid \mathbf{x}^k) = \prod_i p(r_i \mid x_i^k) \tag{2.12}$$

for a memoryless channel, where

$\mathbf{r}$ is the vector of receiver outputs with components r_i and

$\mathbf{x}^k$ is the code symbol vector for the kth trellis path with components x_i^k.

The metrics are obtained as

$$M_k = \ln p(\mathbf{r} \mid \mathbf{x}^k) = \sum_i m_i^k \tag{2.13}$$

where

$$m_i^k = \ln p(r_i \mid x_i^k) \tag{2.14}$$

M_k is the metric for the kth path, and

m_i^k is the metric for the ith code symbol on the kth path.

To accumulate a metric for every possible path through the trellis would be prohibitive, as the number of paths grows exponentially at each stage. The Viterbi algorithm makes use of the fact that paths remerge into each node in groups of 2^b at each stage in the trellis. It is necessary to keep track of only one optimum path leading into each state. The metric for each branch (branch metric) into a given state is added to the accumulated metric (state metric) for the best path into the previous state from which the branch originated. These 2^b metrics are compared, and the best path is retained as the **survivor** into that state. This process is repeated at each stage through the trellis. The maximum likelihood path will never be discarded by this method because none of the paths originating from a given state can accumulate a better metric than the survivor.

The decoder must select a single most likely path in order to deliver an output symbol. If a sufficiently long path history is kept, the 2^ν survivor paths (one for each state) will share a common stem, and the oldest bits corresponding to all the paths will be the same. For the sake of reduced complexity, it is desirable to truncate the path history at some fixed decoding depth. Several authors [12, p. 258; 14, p. 261] have shown that little degradation from optimum performance occurs when the decoding

depth is chosen to be from five to ten times ν, depending on the code rate. The output bits are chosen from the path that currently has the best accumulated metric.

The actual metric used by this decoder may come from either a hard or soft decision receiver. The nature of the metric employed does not affect the operation of the decoder, although it will influence the error performance. For a hard decision receiver, bit decisions are made at the demodulator output, prior to decoding. The negative Hamming distance between the received symbol and the output symbol of each branch is used as the branch metric in this case. The Hamming distance between codewords is generally proportional to the distance between the corresponding signals in the signal space. Thus minimizing the Hamming distance between code vectors, or equivalently maximizing the negative Hamming distance, is the usual hard decision metric. If the added complexity of a soft decision demodulator can be tolerated, then more information is available and the branch metric is proportional to the logarithm of the likelihood function. This results in better error performance.

2.3 Signal Space Mapping

The assignment of codewords to signal points has an important influence on the overall system performance. Previous work on the design of optimal codes has used the Hamming distance between codewords as the distance measure between paths [15, 16]. The Euclidean distance in the signal space between points in the signal constellation actually determines the probability of a transmission error. Ideally, the codewords would be assigned to signal points with Euclidean distance spacings proportional to the Hamming distance of the codewords, so that erroneous decoding into a near neighbour would result in few errors.

Trellis coding [7, 8] considers the actual paths through the trellis when assigning signals. As previously stated, the signal constellation is divided, by a method termed set partitioning, into subsets with maximum spacing between signal points. The signals are assigned to branches in the trellis according to a set of rules that attempts to maximize the Euclidean distance between signal error paths. These rules are as follows

1. all signals should occur with equal frequency and with a fair amount of regularity and symmetry;

2. parallel transitions between states are assigned signals from the subset with maximum signal spacing;

3. transitions originating from the same state are assigned signals from a subset with maximum possible spacing;

4. transitions ending in the same state are assigned signals from a subset with maximum possible spacing.

The papers on trellis coding [7, 8] also recommend that the signal set be expanded to twice the number of points in the uncoded signal set in order to achieve the maximum coding gain without unnecessary complexity.

The multiple tone signal sets which use constant energy orthogonal tones (ie. variable signal energy), form a rectangular constellation as described previously. If each bit of a codeword is mapped onto a different tone, the Euclidean distance between signal points is proportional to the square root of the Hamming distance between codewords.

This situation makes the mapping of codewords onto signal points straightforward, in order to obtain optimum coded performance.

The constant signal energy constellations have an irregular signal spacing, which varies with the number of tones in common between signals. The Euclidean distance between signals cannot be easily mapped onto the Hamming distance between codewords, and so the rules for trellis coding were applied. Set partitioning could not be done in the usual way because of the irregular signal spacings. The signal sets were divided into groups of 2^b (for a rate = b/n code) with maximum spacing between all the members of each subset. All of the codes used have a similar structure, so that the different signal sets may be subdivided the same way. None of the codes have parallel transitions, so that the second rule of trellis coding may be disregarded. The branches in the various trellises diverge and remerge in groups of 2^b according to the rate of the code. For all the optimum codes used, the same group of codewords are associated with the branches that diverge from and remerge into a given state. This allows for the partitioning of the signal sets into groups of 2^b , to produce a desirable mapping onto the codewords. The one exception to this situation is the dual-3 rate 1/2 code used in Case 3B. The same groups of codewords do not appear on the diverging and remerging branches, so that trellis coding rules three and four cannot be satisfied simultaneously. No alternate mapping could be found to improve the spacings between error paths, so the same mapping scheme as for the other rate 3/6 code was employed.

The actual assignment of codewords to signals for the constant signal energy multiple tone constellations are shown in Table 2.2. The codewords are shown as decimal numbers, grouped according to the branch assignments, and the signals are represented by ones and zeroes. Each digit of the signal representation corresponds to

TABLE 2.2

Signal Space Mappings

Case 1B: Rate=2/3, 2 tones, Constant Energy Signals (signalling over 2T)

0	01 01	1	01 11
3	10 01	2	11 01
5	01 10	4	11 10
6	10 10	7	10 11

Case 2C: Rate=2/3, 4 tones, Constant Energy Signals

0	0001	1	0110
3	0010	2	0011
5	0100	4	1001
6	1000	7	1100

Case 3C: Rate=3/6, 8 tones, Constant Energy Signals

0	0001 0000	1	0010 0000	4	0100 0000	5	1000 0000
3	1110 0000	2	1101 0000	7	1011 0000	6	0111 0000
12	1000 0011	13	0100 0011	8	0010 0011	9	0001 0011
15	0100 1001	14	1000 1001	11	0001 1001	10	0010 1001
48	0010 0101	49	0001 0101	52	1000 0101	53	0100 0101
51	1000 1100	50	0100 1100	55	0010 1100	54	0001 1100
60	0100 0110	61	1000 0110	56	0001 0110	57	0010 0110
63	0010 1010	62	0001 1010	59	1000 1010	58	0100 1010
16	0000 0001	17	0000 0010	20	0000 0100	21	0000 1000
19	0000 1110	18	0000 1101	23	0000 1011	22	0000 0111
28	0011 1000	29	0011 0100	24	0011 0010	25	0011 0001
31	1001 0100	30	1001 1000	27	1001 0001	26	1001 0010
32	0101 0010	33	0101 0001	36	0101 1000	37	0101 0100
35	1100 1000	34	1100 0100	39	1100 0010	38	1100 0001
44	0110 0100	45	0110 1000	40	0110 0001	41	0110 0010
47	1010 0010	46	1010 0001	43	1010 1000	42	1010 0100

a tone, and a one indicates a tone which is sent as part of the signal. The use of the signal space mapping described here was compared to an arbitrary mapping scheme for the four tone signal constellation. An improvement of approximately 1.5 dB (E_b/N_0) was obtained for a rate 2/3 code with constraint length of 6.

2.4 Error Performance

The performance of the coded system depends on the structure of the code, the decoding metric, and the coding channel. The coding channel is the effective channel as seen by the encoder and decoder. It includes the properties of the modulator and demodulator, as well as the actual transmission channel. Further details of the following development of error bounds may be found in the references [12, p. 242; 14, p. 243; 21, p. 192; 22].

The first step in obtaining the error performance of the system is to determine the pairwise error probability between two transmitted code vectors. This is the probability that the metric for the error path is larger than the correct path metric for a given received signal sequence, and is expressed by

$$p(\mathbf{x} \rightarrow \hat{\mathbf{x}}) = p\left\{\sum_n m(r_n, \hat{x}_n) \geq \sum_n m(r_n, x_n)\right\} \tag{2.15}$$

The Chernoff bound may be applied to the pairwise error probability to obtain

$$p(\mathbf{x} \rightarrow \hat{\mathbf{x}}) \leq \prod_n E\left\{\exp(\lambda[m(r_n, \hat{x}_n) - m(r_n, x_n)]) \mid x_n\right\} \tag{2.16}$$

For most metrics of interest, the expected value in (2.16) has the form

$$D(\lambda) = E\left\{ \exp(\lambda[m(r_n, \hat{x}_n) - m(r_n, x_n)]) \mid x_n \right\} \tag{2.17}$$

so that

$$p(\mathbf{x} \rightarrow \hat{\mathbf{x}}) \leq [D(\lambda)]^{w(\mathbf{x}, \hat{\mathbf{x}})} \tag{2.18}$$

where $w(\mathbf{x}, \hat{\mathbf{x}})$ is the Hamming distance between $\mathbf{x}$ and $\hat{\mathbf{x}}$ or the number of bits which differ in the two sequences. For the case of an arbitrary metric, the parameter D is given by

$$D = \min_{\lambda \geq 0} D(\lambda) = \min_{\lambda \geq 0} E\left\{ \exp(\lambda[m(r, \hat{x}) - m(r, x)]) \mid x \right\} \Big|_{x \neq \hat{x}} \tag{2.19}$$

When the maximum likelihood metric is used for decoding, ie.

$$m(r, x) = \ln p(r \mid x) \tag{2.20}$$

then one may use the Bhattacharyya parameter

$$Z = \sum_{r} \sqrt{p(r \mid x)\, p(r \mid \hat{x})} \Big|_{x \neq \hat{x}} \tag{2.21}$$

for the value of D.

To obtain the probability of an error event, the union bound is used to give

$$P_E \leq \sum_{j} a(j) D^j \tag{2.22}$$

where

P_E is the probability of an error event

$a(j)$ is the number of error paths of distance j, and

D^j is the pairwise error probability for a path of distance j.

Since the convolutional codes employed are linear, the all zeroes path may be considered as the transmitted sequence, and the coefficients a(j) are obtained from the generating function T(D) to yield

$$P_E \leq T(D) \tag{2.23}$$

with the value of D determined by the coding channel.

The bound on the probability of bit error can be obtained in a similar fashion, and is given by

$$P_B \leq \frac{1}{b} \sum_i \sum_j i\, a(i,j)\, D^j \tag{2.24}$$

where

b is the number of information bits per code symbol,

i is the information weight of the path (ie. the number of bit errors), and

a(i,j) is the number of paths of weight j with information weight i.

The coefficients a(i,j) are the same as in the augmented generating function T(D,I), and the values of i are the same as the exponent of I in each term of the function. The augmented generating function is obtained by equating L to unity in the function T(D,L,I), such as that shown in Figure 2.7. The bit error bound can be written incorporating this function as

$$P_B \leq \frac{1}{b} \frac{\partial T(D, I)}{\partial I}\Big|_{I=1} \tag{2.25}$$

The error bounds presented in this section are used to verify the simulation results for the cases where the coding channel can be easily characterized. The multiple tone signals with variable signal energy form a rectangular signal constellation which can be readily analyzed for coherent reception. The probability of error between two adjacent signals is obtained from the error function

$$p = Q\left(\frac{d}{\sqrt{2N_0}}\right) \tag{2.26}$$

where d is the Euclidean distance between the two signal points. The probability of an error event for a rectangular signal set of n dimensions (ie. n tones) is

$$P_E = 1 - (1 - p)^n \tag{2.27}$$

For the case of hard decision decoding, we may use the Bhattacharryya parameter for an M-ary symmetric channel as the value for D

$$D = \left(\frac{M-2}{M-1}\right)P_E + 2\sqrt{\frac{P_E(1-P_E)}{M-1}} \tag{2.28}$$

The rectangular signal set is not strictly an M-ary symmetric channel, since all of the cross-over probabilities between signals are not equal. However, the error bound still applies in this case.

To obtain an error bound for soft decision decoding, we note that the probability that one code vector is decoded as another code vector is given by

$$P_E(w) = Q\left(\frac{d}{\sqrt{2N_0}}\right) \tag{2.29}$$

where d is again the Euclidean distance between code vectors. The error function may be upper bounded by an exponential function as follows

$$Q\left(\frac{d}{\sqrt{2N_0}}\right) \leq \frac{1}{2} \exp - \frac{d^2}{4N_0} \tag{2.30}$$

For the rectangular signal constellation, the Euclidean distance is proportional to the square root of the Hamming distance, and so we may write

$$d = \sqrt{wE_S} \tag{2.31}$$

where

w is the Hamming distance between the code vectors, and

E_S is the energy of a tone.

Thus the error bound may be rewritten as

$$P_E(w) \leq \frac{1}{2}\left[\exp - \frac{E_S}{4N_0} \right]^w \tag{2.32}$$

To obtain the bound for the overall probability of an error event, we sum the individual components over w to yield

$$\begin{aligned} P_E &= \sum_w P_E(w) \\ &\leq \sum_w \frac{1}{2}\, a(w) \left[\exp - \frac{E_S}{4N_0} \right]^w \\ &= \frac{1}{2} T(D) \Big|_{D = \exp - \frac{E_S}{4N_0}} \end{aligned} \tag{2.33}$$

These two values for the parameter D may also be used to find the bound on the bit error probability for coherent demodulation of coded rectangular signal sets. Equation (2.24) or (2.25) may be used, with a multiplying factor of one half in the soft decision case. The bit error bounds were computed for the various codes used with multiple tone signals with fixed signal energy per orthogonal component (ie. constant energy tones). These bounds are plotted with the corresponding simulation results in the appropriate subsections of the next chapter. The performance of coding with constant signal energy constellations and coherent demodulation, and the performance of all the coded systems employing noncoherent reception are not easily evaluated. Just as the error probability for uncoded transmission was difficult to obtain, the evaluation of the bound parameter D is not tractable for these cases.

CHAPTER THREE

RESULTS

3.1 Overview

3.1.1 Program Description

The simulation program used to model the communication system was written in FORTRAN, and run on both VAX 11/750 and IBM 3081 computers. The program is divided into a mainline routine, which handles the initialization, input, and output tasks, and several subroutines which correspond to the various components of the system. The input file for the simulation contains the parameters of the code, which are the rate, the constraint length, and the generator matrix. A look-up table of output symbols corresponding to various branches in the trellis is generated by an initialization subroutine. This table is used by the encoding and decoding subroutines. The type of demodulation (coherent/noncoherent), and whether hard or soft decisions are to be made, are also indicated in the input file. The different signal space mappings are obtained by using different versions of the channel subroutine, which will be described later.

After the initialization procedures are complete, the main program commences by generating a random bit stream. This is done with a library subroutine for pseudorandom number generation. The information symbols are passed to the encoder subroutine which returns the encoded data symbols. These data symbols are passed to the channel subroutine which simulates the modulator, the AWGN channel, and the

demodulator. In each signalling interval, the subroutine calculates and returns a metric for each member of the signal space. These metrics are then passed to the decoding subroutine, which constructs the received bit stream. The main program compares the received data to the original information bits, and keeps track of the errors. Error events, symbol errors, and bit errors are all tabulated. The signal to noise ratio (SNR) starts at one dB and is incremented in steps of one dB. One hundred thousand data symbols are simulated at each level of SNR. After each set of data points is processed, the three error probabilities are calculated and sent to a data file along with the SNR value. The SNR is then incremented and the procedure repeats until the error event count is less than ten in one hundred thousand data points at the given SNR. The output data file is used to plot error performance curves which appear later in this chapter.

The encoder subroutine preserves the previous input bits which determine the state of the encoder. The current information symbol then determines the transition to the next state and the corresponding output symbol. This is accomplished by using the present state and input bits as an index to the table generated during initialization. The output symbol is contained in the table, and is returned to the mainline by the encoder subroutine.

The channel subroutine receives the data symbol and several parameters of the modulation scheme. The SNR level, the type of demodulation (coherent/noncoherent), and the type of decoding metric (hard/soft) are all passed from the mainline. Different versions of the channel subroutine are used to accommodate the various signal space mappings in the simulations of the different cases. Given the transmitted signal and the SNR value, a decision variable is computed for each member of the signal space.

Samples of Gaussian noise are calculated from uniformly distributed pseudorandom numbers, according to the polar formula [6].

$$X_1 = V_1 \sqrt{-\frac{2 \ln S}{S}} \tag{3.1}$$

and

$$X_2 = V_2 \sqrt{-\frac{2 \ln S}{S}} \tag{3.2}$$

are two independent samples of a zero mean, unit variance, normally distributed random variable, where

$$S = V_1^2 + V_2^2 \tag{3.3}$$

and S must be less than unity.

$$V_1 = 2U_1 - 1 \tag{3.4}$$

and

$$V_2 = 2U_2 - 1 \tag{3.5}$$

where U_1 and U_2 are samples of a random variable, uniformly distributed between zero and one. A random phase angle is added to the transmitted signal for the case of noncoherent reception. The angle (θ) is assumed to be uniformly distributed between zero and two pi radians, and is obtained from a pseudorandom number generated by the library subroutine. For soft decisions, the actual decision variables are returned to the main program as decoder metrics. The data symbol corresponding to the largest decision variable is determined in order to calculate the hard decision metric. The negative Hamming distance between the demodulated symbol and the branch symbol is

returned as the branch metric in this case. Details of the demodulation and metric calculation are given in Chapter two.

The decoder subroutine implements the Viterbi algorithm. A bit history and path metric are maintained for each state of the code. At each signal interval, the metric for the signal corresponding to each transition in the trellis is added to the path metric for the originating state of that branch. The paths entering each state are compared, and the one with the largest metric is retained as the survivor. This process makes use of the look-up table of trellis states and transitions, and the information symbols for the bit histories also come from the table. The output bits are taken from the bit history corresponding to the path with the largest metric at each step. The length of the history maintained by the decoder varies with the code constraint length and code rate according to the formula

$$L = 5b\nu \tag{3.6}$$

where

L is the length of the bit history,

ν is the code constraint length, and

b is the information bit rate (code rate = b/n).

This decoder has negligible performance degradation due to path history truncation. Clark and Cain [14, p. 262] suggest that path histories for near optimal decoder operation should be 5ν for rate 1/2 codes, 8ν for rate 2/3 codes, and 10ν for rate 3/4 codes.

TABLE 3.1

Case Descriptions

CASE	INFORMATION RATE	CODE RATE	CONSTRAINT LENGTHS	NUMBER OF TONES	NUMBER OF SIGNALS	E_{peak}/E_{av}
1A	1 bit/T	1/2	2, 6	2	4	2.0
1B	1 bit/T	2/3	4, 6	2	8	1.0
2A	2 bits/T	2/3	4, 6	3	8	2.0
2B	2 bits/T	2/4	6	4	16	2.0
2C	2 bits/T	2/3	4, 6	4	8	1.0
3A	3 bits/T	3/4	5	4	16	2.0
3B	3 bits/T	3/6	3, 6	8	64	1.0

NUMBER OF TONES = BANDWIDTH $\times$ 2T

3.1.2 Case Summary

There are seven different coding and modulation schemes considered in this report. The characteristics of each scenario, and the numbering scheme used to disinguish them, are shown in Table 3.1. They are divided into three groups, and the number of the case indicates the number of information bits transmitted per signalling interval. There is also a letter associated with each case to differentiate the different code rates and modulation schemes employed.

Four of the cases (1A, 2A, 2B, 3A) use signals which may contain any combination of tones. These signals have a variable signal energy, depending on the number of tones in the signal. They are compared to the baseline system according to average signal energy. For example, let E_S be the energy of a single tone. For the four tone case, there are sixteen signals with average signal energy given by

$$E_{av} = \frac{1(0) + 4(E_S) + 6(2E_S) + 4(3E_S) + 1(4E_S)}{16} = 2E_S \tag{3.7}$$

Therefore, the signal energy of this system is reduced by 1/2 for comparison with the baseline system, which has a signal energy of E_S. The other variable signal energy cases are also scaled appropriately. The remaining three cases (1B, 2C, 3B) have constant energy signals, with signal energy equal to the energy of a single tone, for direct comparison with the baseline system.

Each of the seven cases has several sets of results. The various systems were all simulated with both coherent and noncoherent demodulation, both hard and soft decoding metrics, and different code constraint lengths. All of the simulation results for each case appear on two figures, one for coherent reception and one for noncoherent

reception, each with the corresponding baseline system performance curve. The measure of performance on the graphs is the bit error rate (BER) plotted against the energy per bit to noise spectral density ratio (E_b/N_0). As mentioned previously, the error events and symbol errors as well as the signal energy to noise ratio were tabulated by the simulation program, but the bit error performance was chosen as the most suitable criterion for comparison. Table 3.2 shows the required E_b/N_0 to give a BER of 10^{-4} for every case simulated. These values were obtained from the figures shown later in this chapter, with some extrapolation required on some of the curves. For data transmission, system performance at a BER of 10^{-5} or less is usually of most interest. However, the simulation run time to obtain reliable data in this region is prohibitive. Some curves display irregular behaviour for the last data point (ie. the lowest BER point). This occurs because the BER is calculated using a very small number of error events, and the random occurrence of a single error causes a large displacement of the point on the graph. Since error performance curves are known to behave smoothly at low BER values, these points are neglected when extrapolating the curves. All performance values quoted in this chapter will refer to E_b/N_0 in dB at the reference BER of 10^{-4}.

As a verification of the simulation program performance, several test cases were run and compared to theoretical results. The baseline systems (2, 4, and 8-ary FSK) were simulated for both coherent and noncoherent demodulation, and the results matched closely with the theoretical performance. The modulation scheme which uses all possible tone combinations to obtain a rectangular signal set of 2^M signals from M orthogonal tones was also simulated for the various values of M. The performance of this system, with no coding and coherent demodulation, reflected the theoretical error probabilities for rectangular signal constellations. In both cases, the error performance curves for the simulation matched the theoretical results to within one-half dB over the entire curve. In

TABLE 3.2

Coherent Results

CASE	BASELINE PERFORMANCE	HARD DECISION PERFORMANCE	SOFT DECISION PERFORMANCE
1A	11.5	9.7 ($\nu = 2$), 8.3 ($\nu = 6$)	8.2 ($\nu = 2$), 6.4 ($\nu = 6$)
1B	11.5	12.6 ($\nu = 4$), 12.1 ($\nu = 6$)	9.7 ($\nu = 4$), 9.4 ($\nu = 6$)
2A	8.8	9.2 ($\nu = 4$), 9.3 ($\nu = 6$)	7.5 ($\nu = 4$), 7.0 ($\nu = 6$)
2B	8.8	9.9 ($\nu = 6$)	7.4 ($\nu = 6$)
2C	8.8	9.7 ($\nu = 4$), 9.5 ($\nu = 6$)	7.3 ($\nu = 4$), 6.8 ($\nu = 6$)
3A	7.4	9.3 ($\nu = 5$)	7.2 ($\nu = 5$)
3B	7.4	11.7 ($\nu = 3$), 9.9 ($\nu = 6$)	7.7 ($\nu = 3$), 5.0 ($\nu = 6$)

Noncoherent Results

CASE	BASELINE PERFORMANCE	HARD DECISION PERFORMANCE	SOFT DECISION PERFORMANCE
1A	12.3	10.8 ($\nu = 2$), 9.4 ($\nu = 6$)	9.2 ($\nu = 2$), 7.7 ($\nu = 6$)
1B	12.3	12.8 ($\nu = 4$), 12.4 ($\nu = 6$)	10.5 ($\nu = 4$), 10.0 ($\nu = 6$)
2A	9.6	10.1 ($\nu = 4$), 9.4 ($\nu = 6$)	8.1 ($\nu = 4$), 7.5 ($\nu = 6$)
2B	9.6	10.1 ($\nu = 6$)	8.0 ($\nu = 6$)
2C	9.6	10.0 ($\nu = 4$), 9.9 ($\nu = 6$)	7.6 ($\nu = 4$), 6.9 ($\nu = 6$)
3A	8.2	9.6 ($\nu = 5$)	7.7 ($\nu = 5$)
3B	8.2	12.0 ($\nu = 3$), 10.0 ($\nu = 6$)	7.8 ($\nu = 3$), 5.8 ($\nu = 6$)

coded systems which employ the rectangular signal constellations, error bounds were calculated as described in section 2.4. The coherent simulation results with their respective error bounds are shown in the appropriate subsections of this chapter.

3.2 Simulation Results

3.2.1 Case 1A: Rate = 1/2, 2 tones, Variable Signal Energy

This case has the best results of those investigated. All of the coded systems outperform the baseline by between 1.5 and 5.1 dB at the reference BER of 10^{-4}. The number of points in the signal space is doubled by the use of multiple tone signals so that optimal rate 1/2 codes can be employed. This provides a redundant coded bit for each bit of information transmitted, and thus good error correction ability. The two codes used in the simulation have constraint lengths of 2 and 6 with free distances of 5 and 10 respectively. The longer code is quite common, and has been used in other satellite applications [19].

The results for coherent reception are shown in Figure 3.1. The improvement over the baseline system ranges from 1.8 dB for the short code with hard decisions, to 5.1 dB for the long code with soft decisions. The use of soft decisions provides a gain of 1.5 dB over hard decisions for the short code, yielding a margin of 3.3 dB over the baseline. A 1.9 dB improvement, from 3.2 dB better than the reference with hard decisions to a 5.1 dB advantage with soft decisions, is obtained for the longer code. For hard decisions, the effect of increasing the constraint length from 2 to 6 yields 1.4 dB improvement, and 1.8 dB is gained in the soft decision case.

The performance of the noncoherent receiver appears in Figure 3.2. The results are very similar to the coherent case, with 1.5 to 4.6 dB of improvement over the baseline system. The short constraint length code provides a 1.5 dB advantage with hard decisions, and an additional 1.6 dB gain for soft decisions. Increasing the code constraint length enhances performance by 1.4 dB for a 2.9 dB improvement on the baseline with hard decisions, and by 1.5 dB in the soft decision case.

The theoretical error bounds for the two codes are also shown. Figure 3.3 shows the bound for the shorter code, and the longer code appears in Figure 3.4.

3.2.2 Case 1B: Rate = 2/3, 2 tones, Constant Signal Energy (signalling over 2T)

Case 1B uses a rate 2/3 optimal code with the three bit codewords sent over two signalling intervals. There is less redundant information in the data stream, and so the performance is understandably worse than Case 1A. The advantage to this scenario is that the signals have constant energy. In this case, the computation of the decision variables is simplified. However, the Euclidean distance between the signals is smaller in this case than in the previous modulation scheme, which is detrimental to error performance. Codes with constraint lengths of 4 and 6 and corresponding free distances of 5 and 7 were simulated.

For the coherent receiver, the worst case coded system is 1.1 dB worse than the baseline performance, as shown in Figure 3.5. This is the short constraint length code with hard decisions. Increasing the constraint length yields only 0.5 dB improvement but soft decisions provide larger gains. The short constraint length code with soft decisions gives 1.8 dB improvement over the baseline system, which is 2.9 dB better than the hard

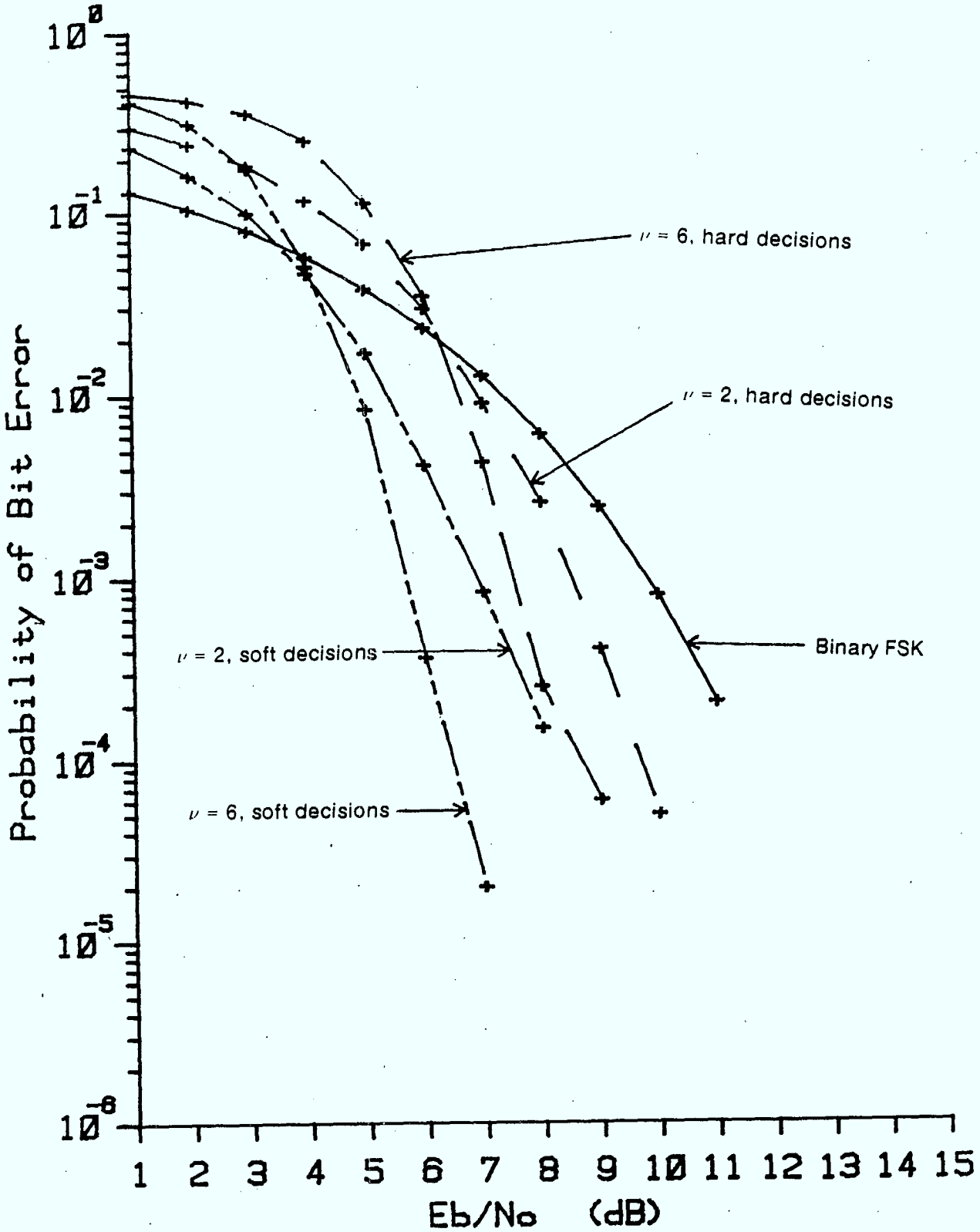

Figure 3.1 Case 1A Simulation Results, Coherent Reception

Rate = 1/2, 2 tones, Variable Signal Energy

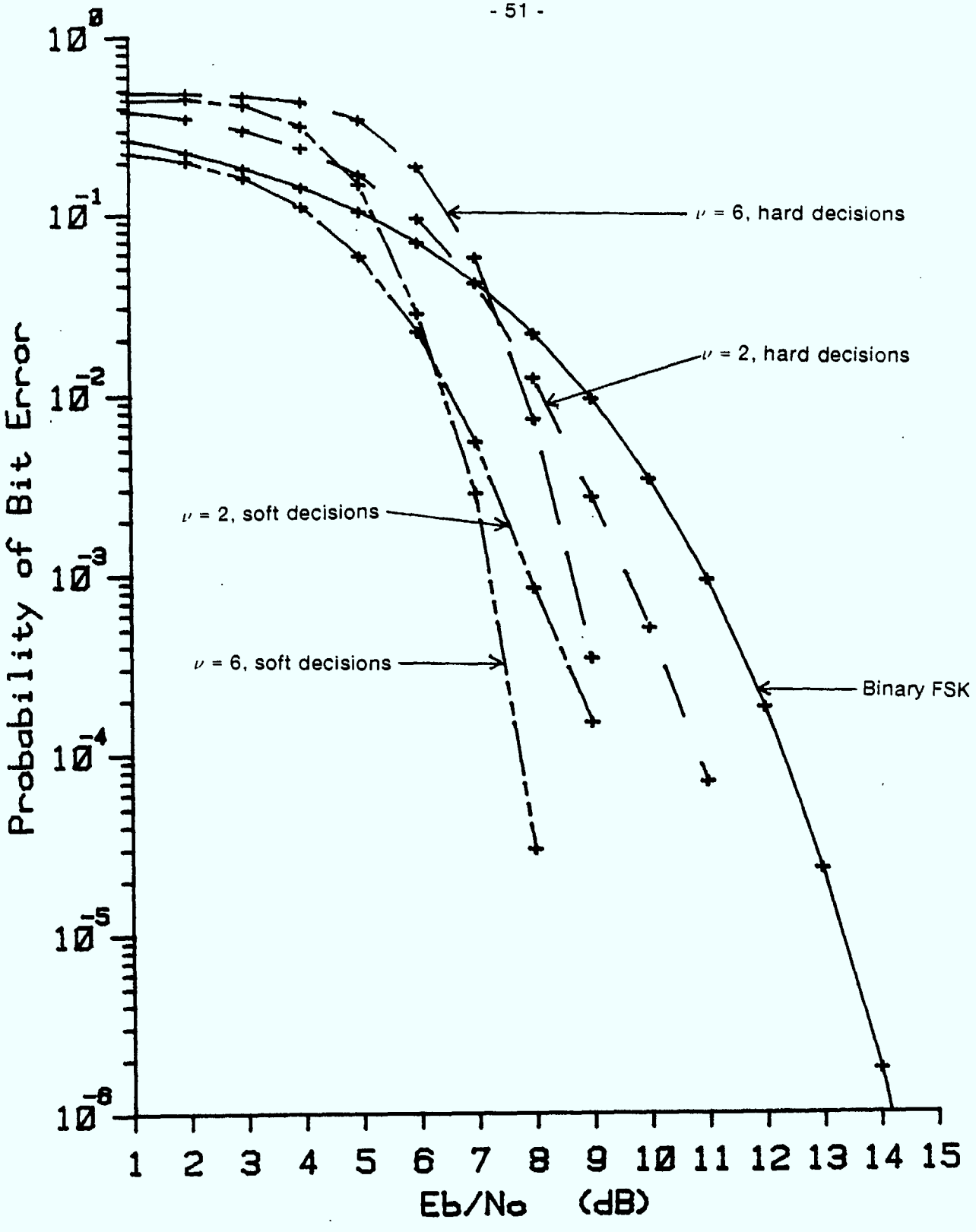

Figure 3.2 Case 1A Simulation Results, Noncoherent Reception

Rate = 1/2, 2 tones, Variable Signal Energy

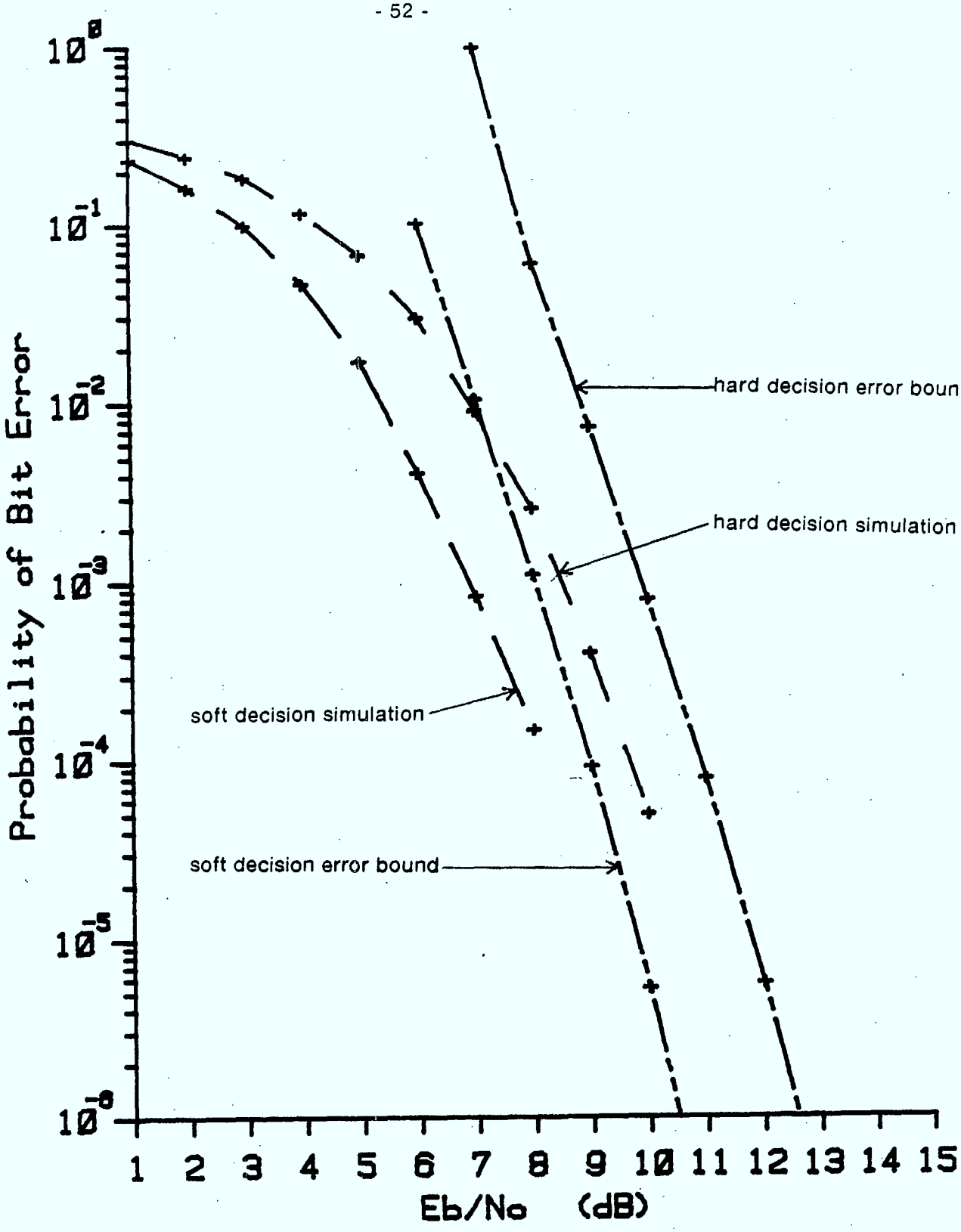

Figure 3.3 Case 1A Code Error Bounds (ν = 2), Coherent Reception

Rate = 1/2, 2 tones, Variable Signal Energy

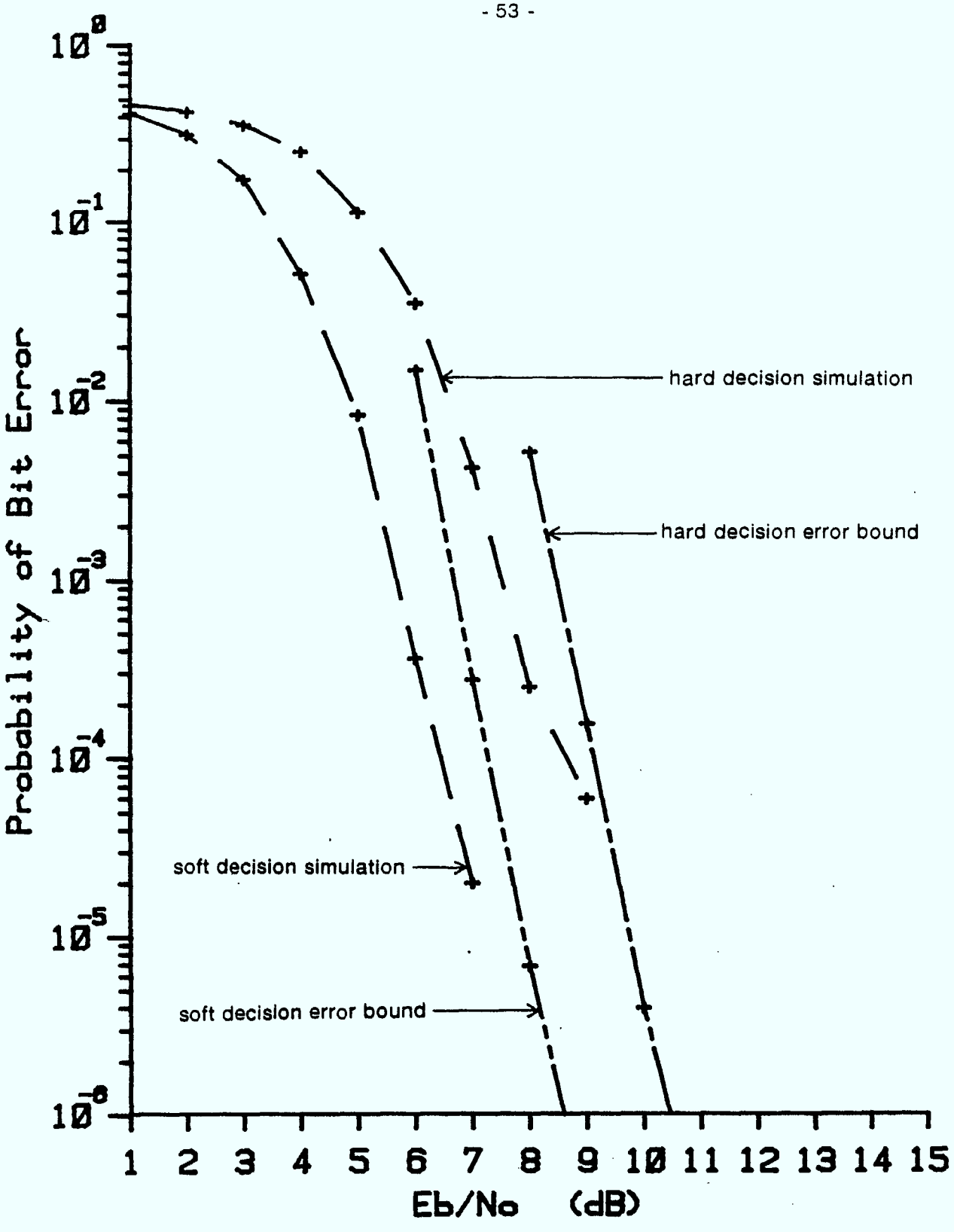

Figure 3.4 Case 1A Code Error Bounds (ν = 6), Coherent Reception

Rate = 1/2, 2 tones, Variable Signal Energy

decision case. The longer constraint length again provides a very modest additional gain of 0.3 dB.

The noncoherent system has performance curves very similar to the coherent case, and they are shown in Figure 3.6. The hard decision simulations are worse than the baseline by 0.5 and 0.1 dB for the short and long constraint length codes respectively. Using soft decisions yields 2.3 to 2.4 dB of improvement over hard decisions. This results in 1.8 dB improvement over the baseline for the shorter code, and 2.3 dB gain for the longer code.

In all situations, the coded system performance curves are steeper than that of the baseline. This implies that the hard decision performance will approach or even surpass the baseline system at higher SNR levels. As well, the soft decision improvement will increase as the curves diverge. This additional improvement will not be very large, probably less than one dB. The difference in slope of the curves also means that the baseline system surpasses the performance of the soft decision coded system at low SNR values. This happens below the point where the curves intersect, known as the cross-over point. The cross-over point occurs at E_b/N_0 of 7.8 dB for coherent reception and 8.5 dB in the noncoherent case.

3.2.3 Case 2A: Rate = 2/3, 3 tones, Variable Signal Energy

This is the first case which has an information rate of two bits per signalling interval, corresponding to a baseline system of 4-ary FSK. A rate 2/3 code is used, which requires an eight point signal space. Three tones are employed, with all combinations of tones allowed, to provide eight variable energy signals. The two codes used in the

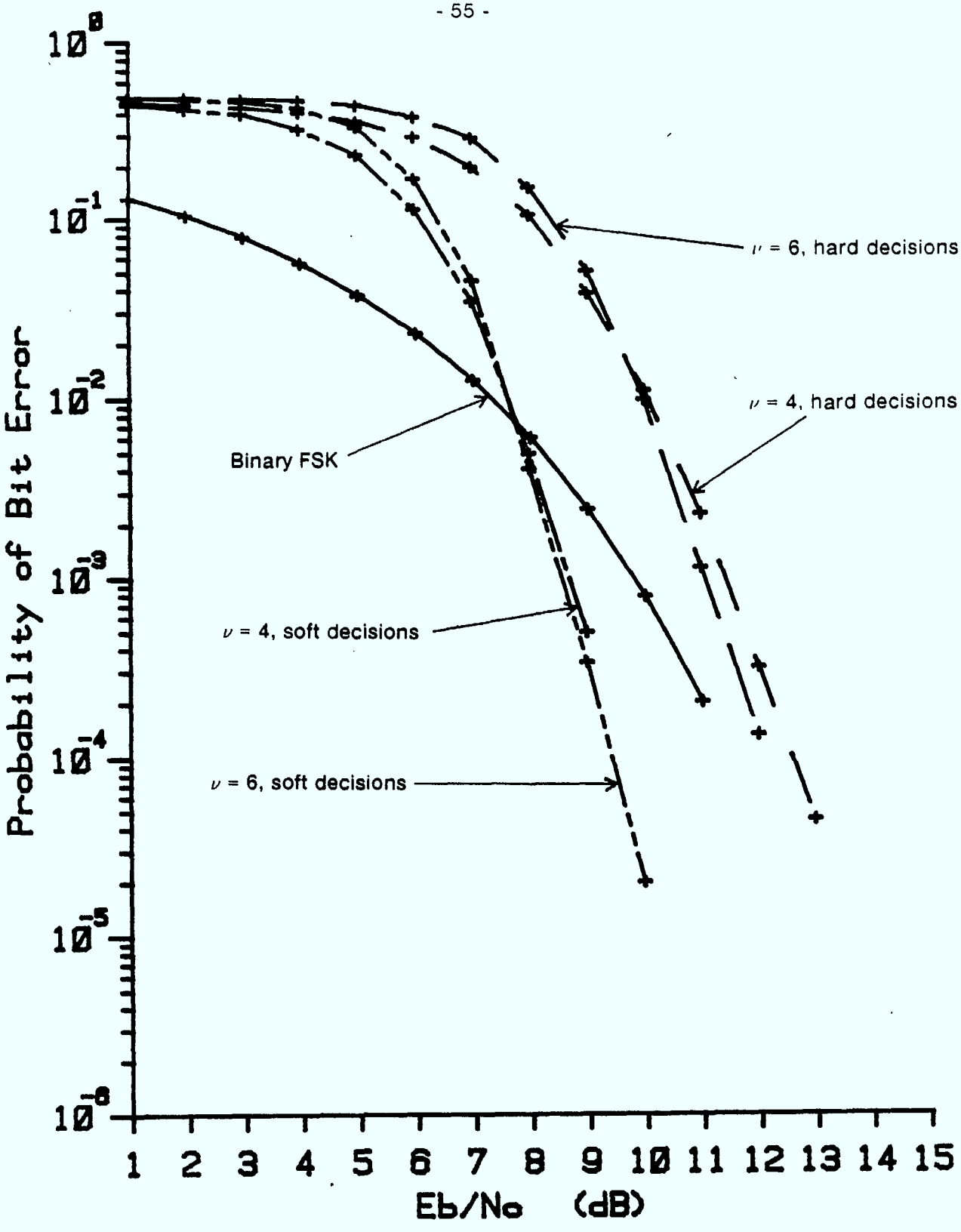

Figure 3.5 Case 1B Simulation Results, Coherent Reception

Rate = 2/3, 2 tones, Constant Signal Energy (signalling over 2T)

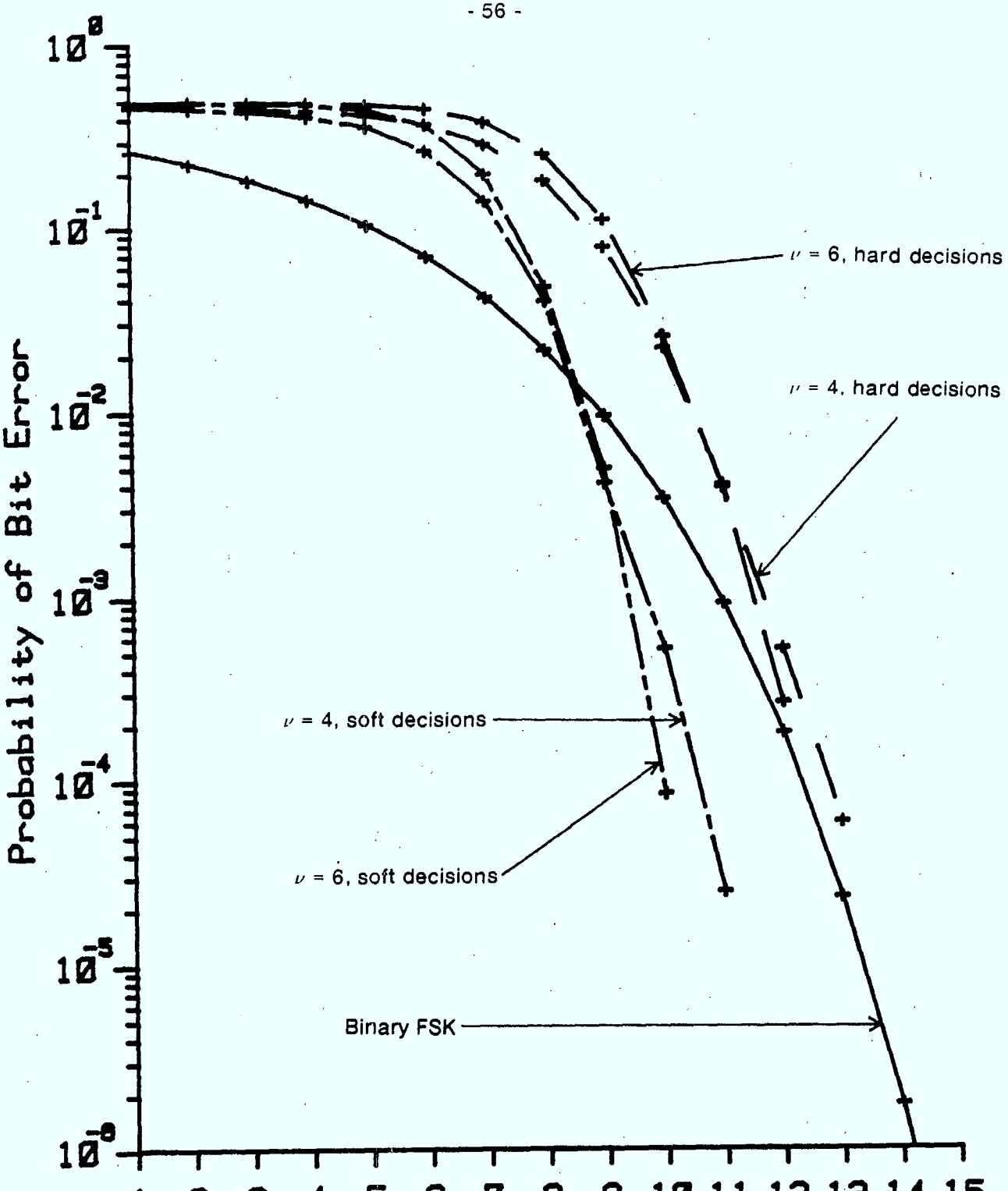

Figure 3.6 Case 1B Simulation Results, Noncoherent Reception

Rate = 2/3, 2 tones, Constant Signal Energy (signalling over 2T)

simulation are the same as those in the previous case, with constraint lengths of 4 and 6.

The results for coherent reception are shown in Figure 3.7. The performance of both codes is virtually identical with hard decision decoding, and is about 0.5 dB worse than the baseline system. Soft decision decoding yields 1.3 dB improvement over the reference system for the short constraint length code, and an additional 0.5 dB for the longer code. The cross-over points for the soft decision curves are between 5.5 and 6.0 dB (E_b/N_0).

Figure 3.8 displays the performance curves for noncoherent reception of Case 2A. The short constraint length code with hard decisions is 0.5 dB worse than the baseline, while the longer code is 0.2 dB better than the reference system. The use of soft decisions yields about 2 dB of improvement over the hard decision case. The performance gain over the baseline with the soft decision decoder is 1.5 dB for the shorter code, and 2.1 dB for the longer constraint length code. Both soft decision curves intersect the baseline curve at 6.3 dB on the horizontal axis.

This case achieves performance improvements with a reduction in required bandwidth. The spacing between orthogonal tones is the same for the three tone coded system and the four tone baseline system. The coded signals therefore require only 3/4 of the bandwidth, although a higher peak power transmitter is neccessary for the multiple tone signals. It is also significant to note the free distances of the optimal rate 2/3 codes. The shorter code ($\nu = 4$) has a free distance of 5, while the longer code ($\nu = 6$) has a free distance of 7. These parameters will be used for comparison between the different cases at this information rate.

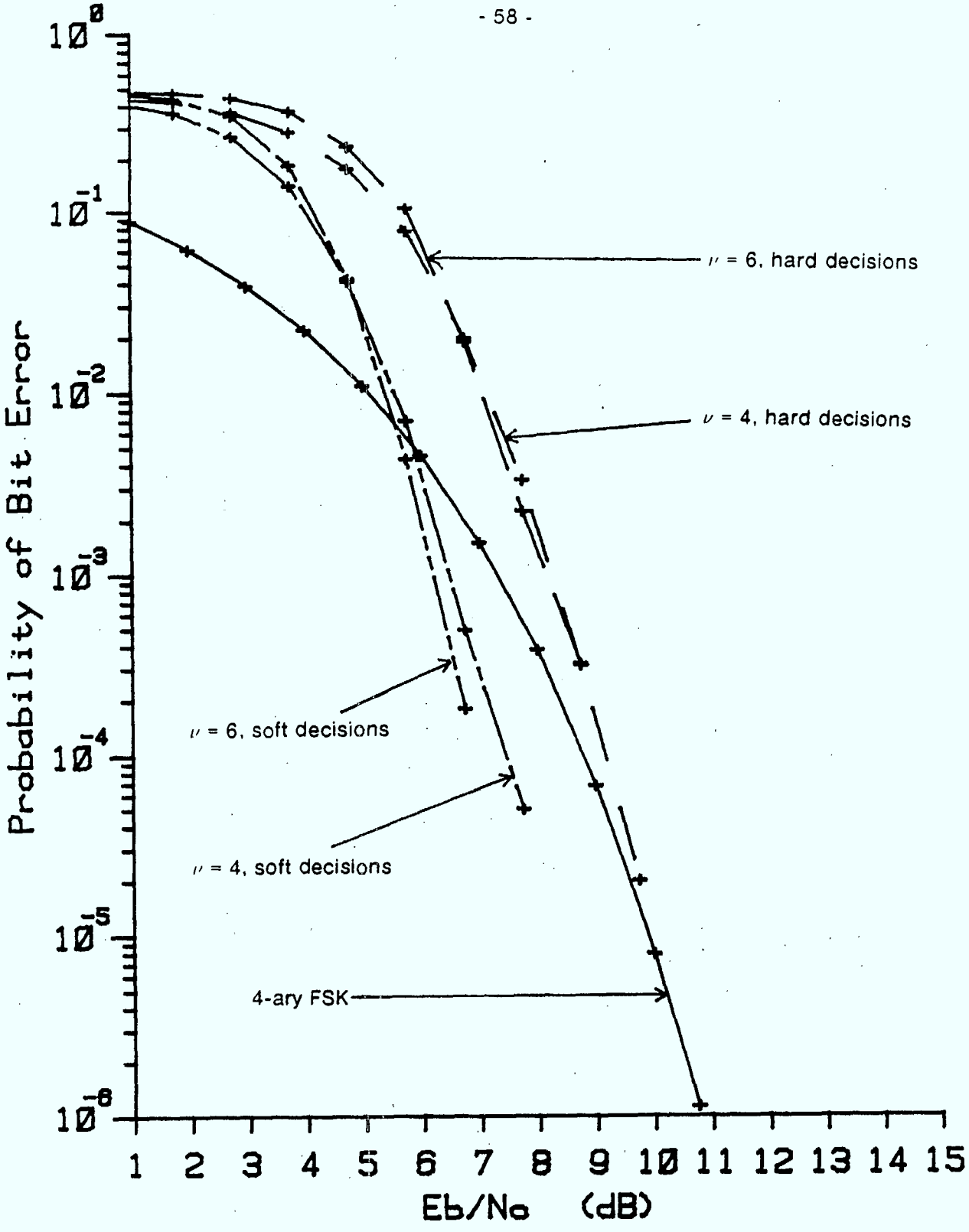

Figure 3.7 Case 2A Simulation Results, Coherent Reception

Rate = 2/3, 3 tones, Variable Signal Energy

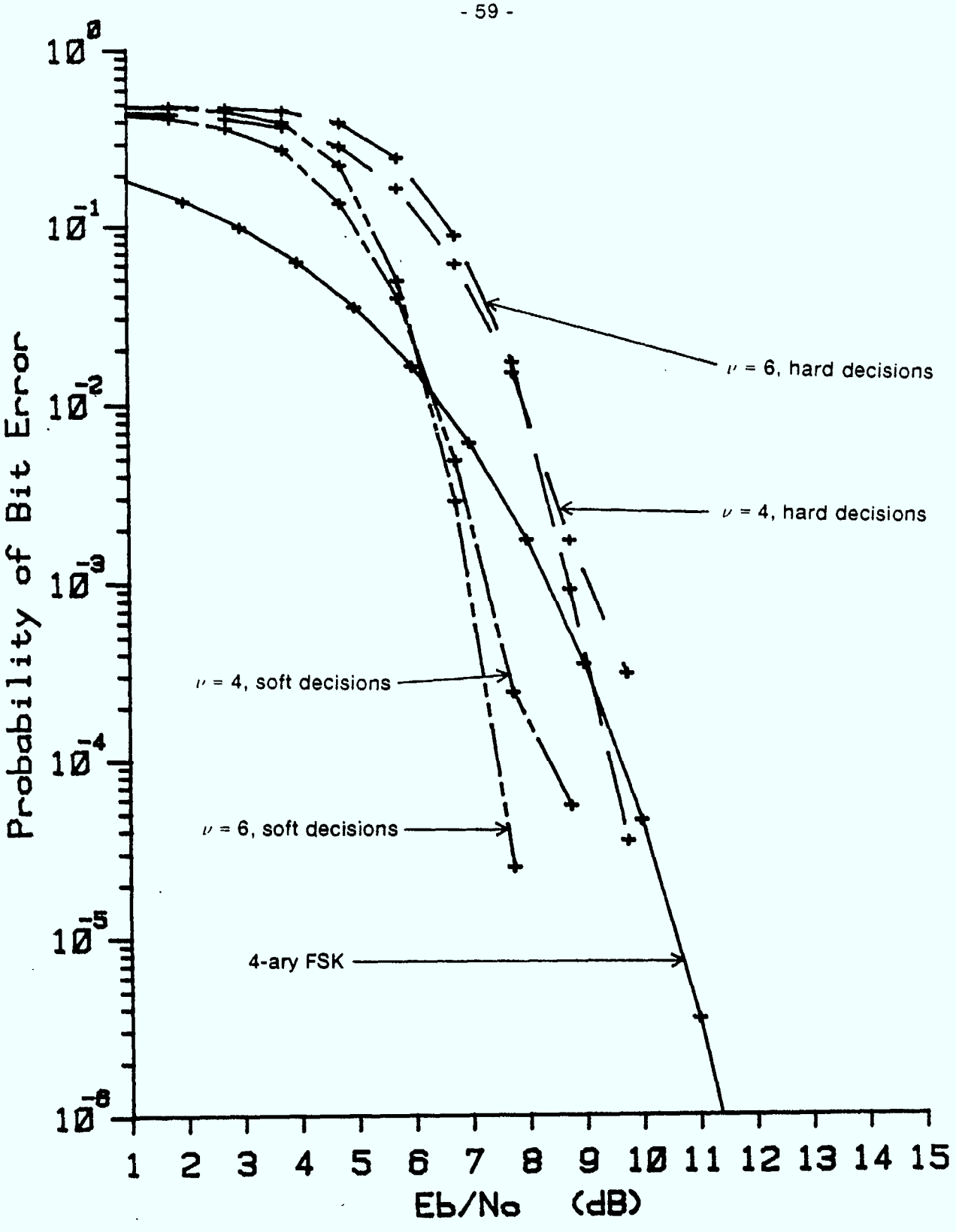

Figure 3.8 Case 2A Simulation Results, Noncoherent Reception

Rate = 2/3, 3 tones, Variable Signal Energy

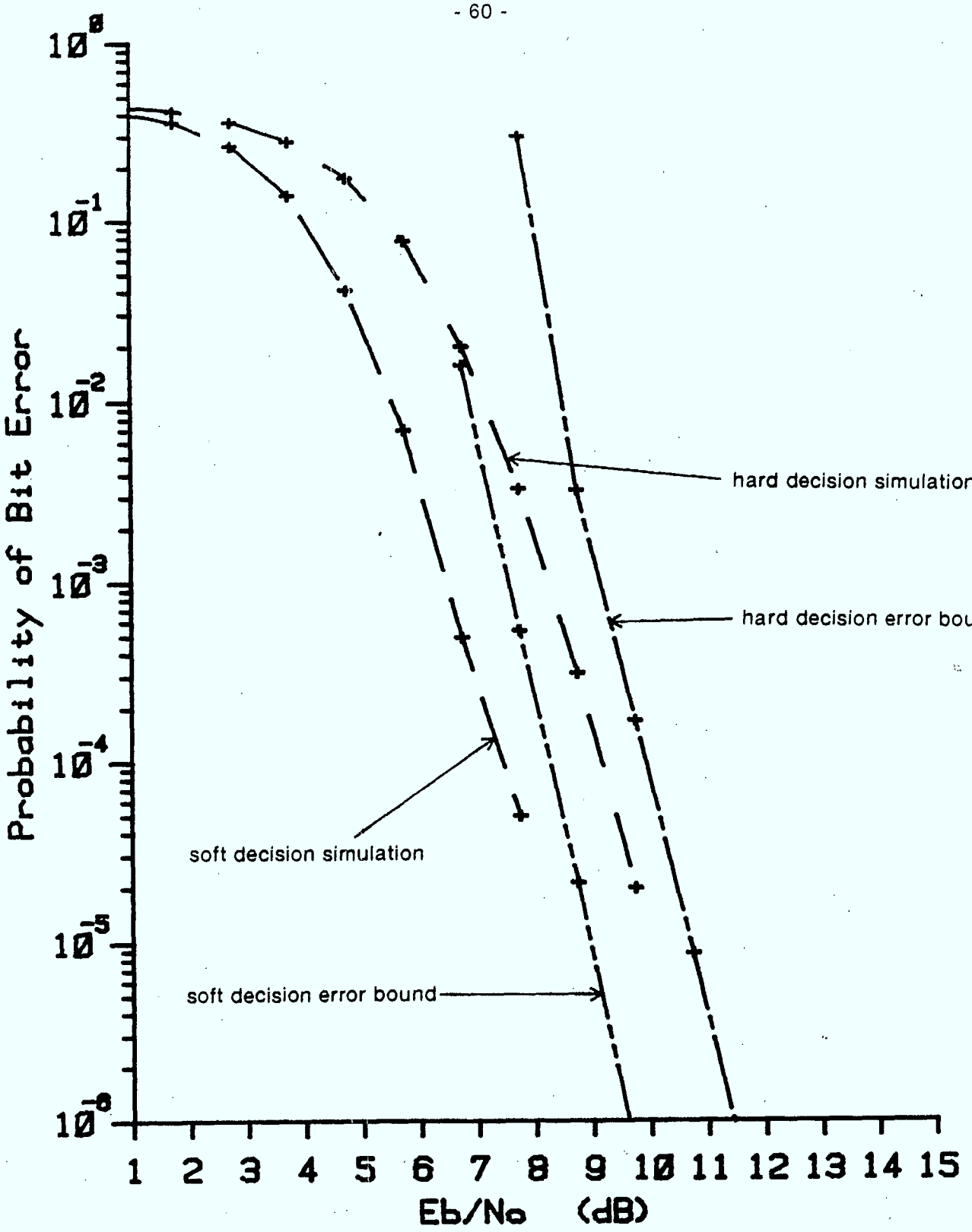

Figure 3.9 Case 2A Code Error Bounds (ν = 4), Coherent Reception

Rate = 2/3, 3 tones, Variable Signal Energy

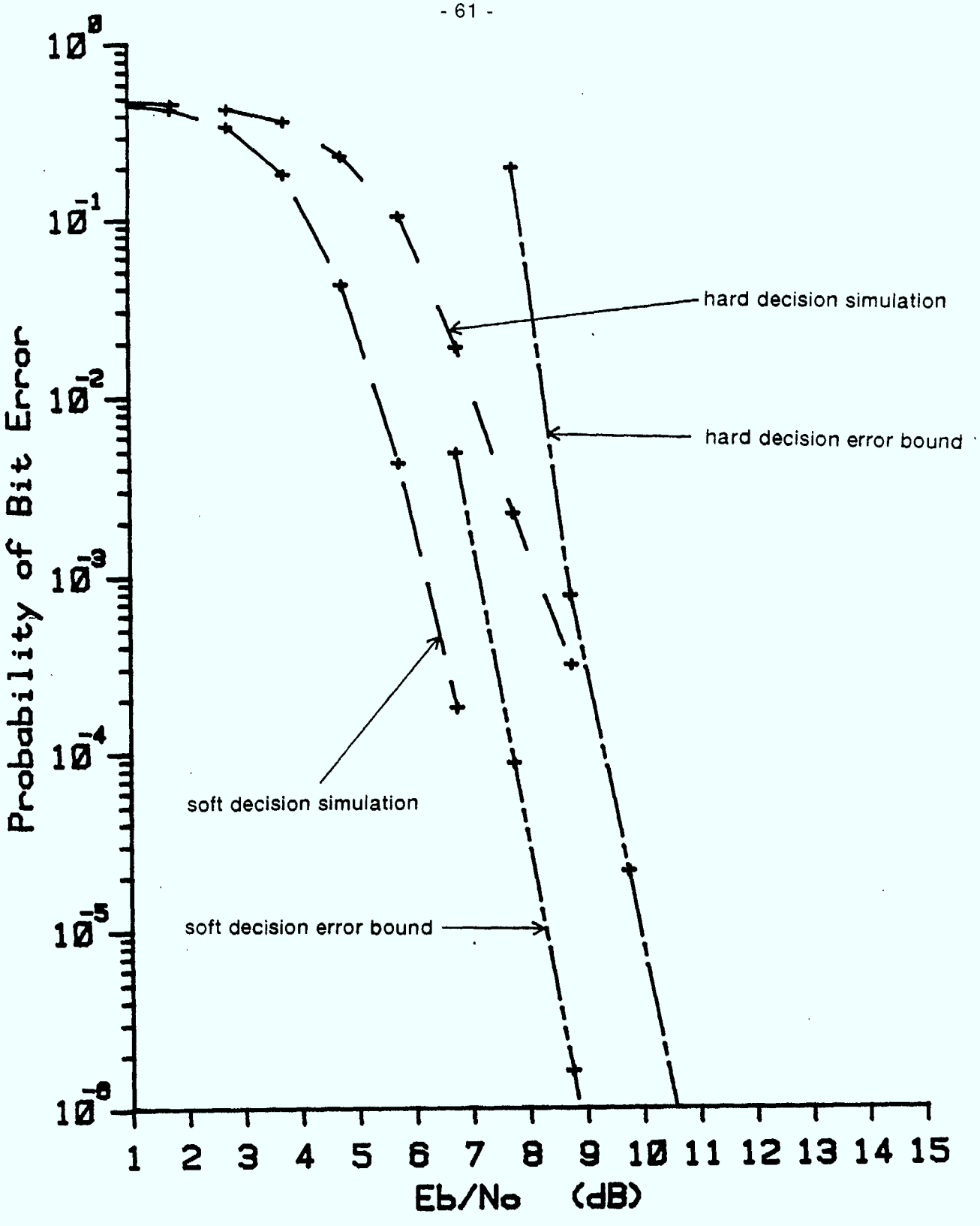

Figure 3.10 Case 2A Code Error Bounds (ν = 6), Coherent Reception

Rate = 2/3, 3 tones, Variable Signal Energy

There are two figures which display the theoretical error bounds for coded performance with rectangular signal constellations, as described in Chapter two. Figure 3.9 shows the bound for the shorter code and Figure 3.10 contains the results for the longer constraint length code.

3.2.4 Case 2B: Rate = 2/4, 4 tones, Variable Signal Energy

This case employs all four tones in the coded system that are used in the baseline FSK modulation. All tone combinations are used to provide sixteen signals with signal energies that depend on the number of constituent tones. The code for this case has rate 2/4 to provide a four bit codeword for two bits of information in each signalling interval. An optimum distance profile code of this rate could not be found in the literature, and so two identical rate 1/2 encoders in parallel were used. Only one code was simulated, with a constraint length of 6, composed of two rate 1/2 codes of constraint length 3.

The performance of the coherent reception system is shown in Figure 3.11. With hard decisions, the coded simulation is 1.1 dB worse than the baseline. Soft decisions yield a 2.5 dB gain to provide 1.4 dB improvement over the reference system. Figure 3.12 displays the performance curves for the noncoherent receiver. The soft decision decoder is superior to the baseline system by 1.6 dB while the hard decision curve is 0.5 dB worse than 4-ary FSK.

The performance of the coded system in this case is virtually the same as the previous case in spite of the lower rate code and increased signal bandwidth. The reason for this is that the code structure employed does not take full advantage of the signal space. The code formed by two cascaded rate 1/2 encoders has double the constraint length of a single component code yet only achieves the same free distance.

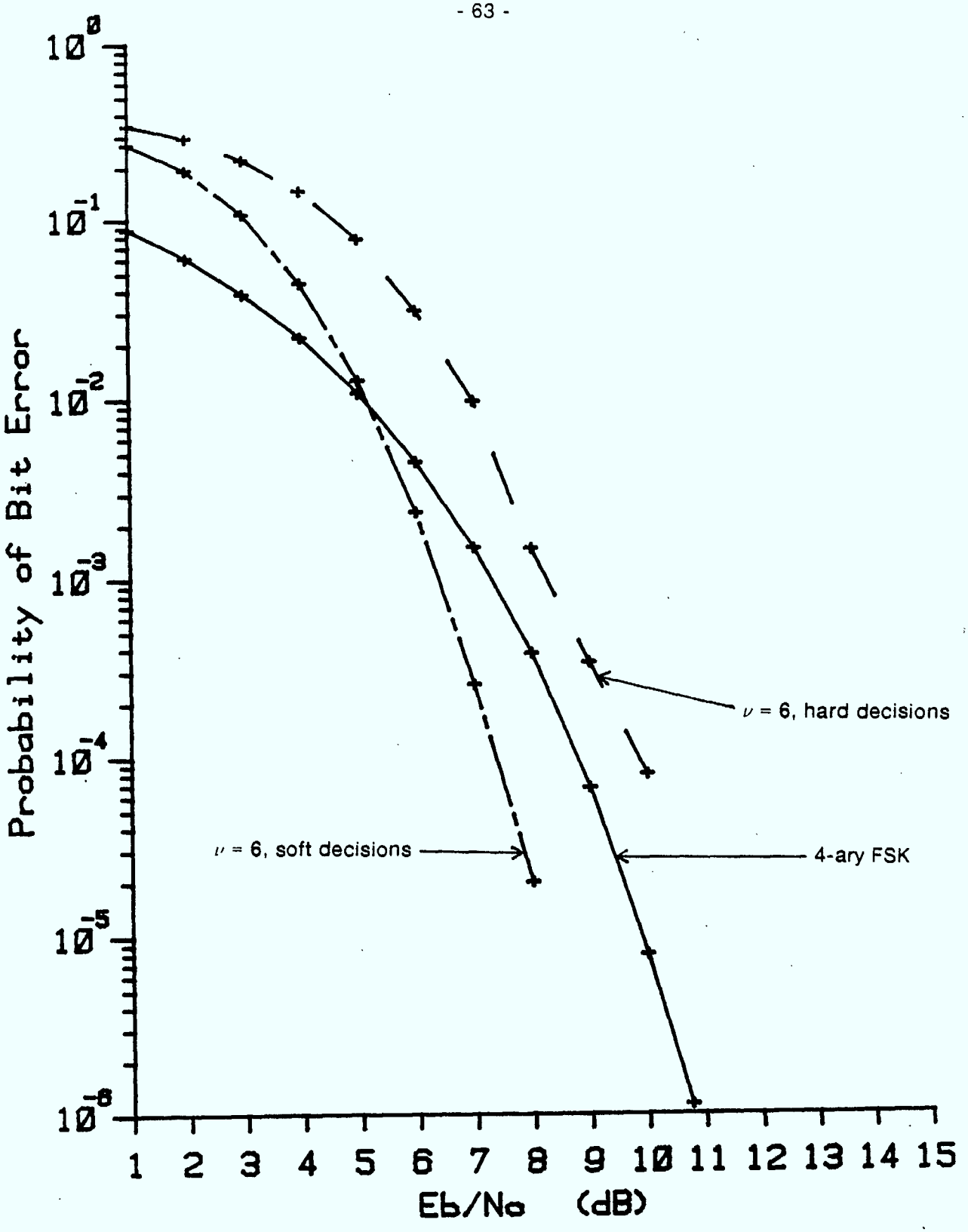

Figure 3.11 Case 2B Simulation Results, Coherent Reception

Rate = 2/4, 4 tones, Variable Signal Energy

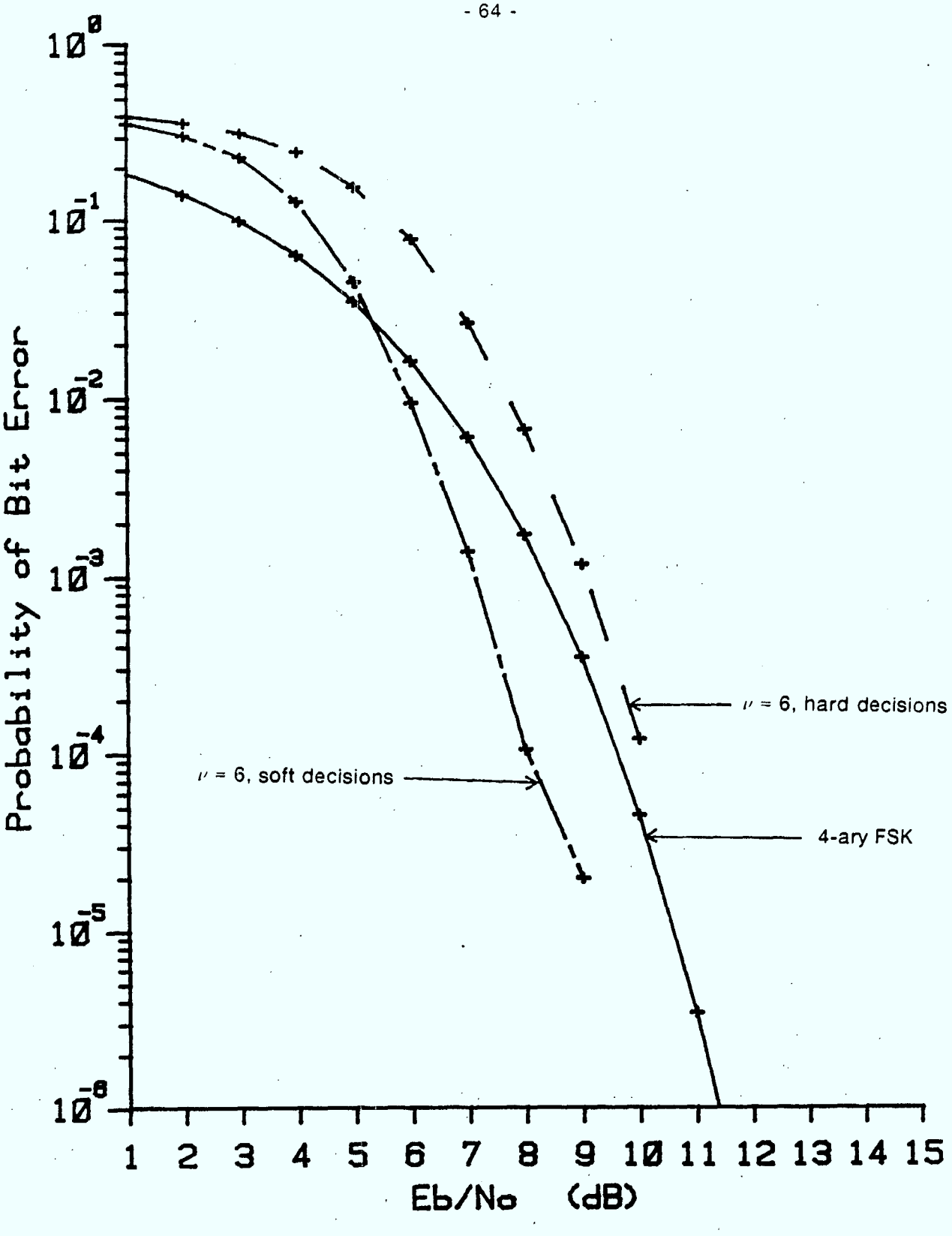

Figure 3.12 Case 2B Simulation Results, Noncoherent Reception

Rate = 2/4, 4 tones, Variable Signal Energy

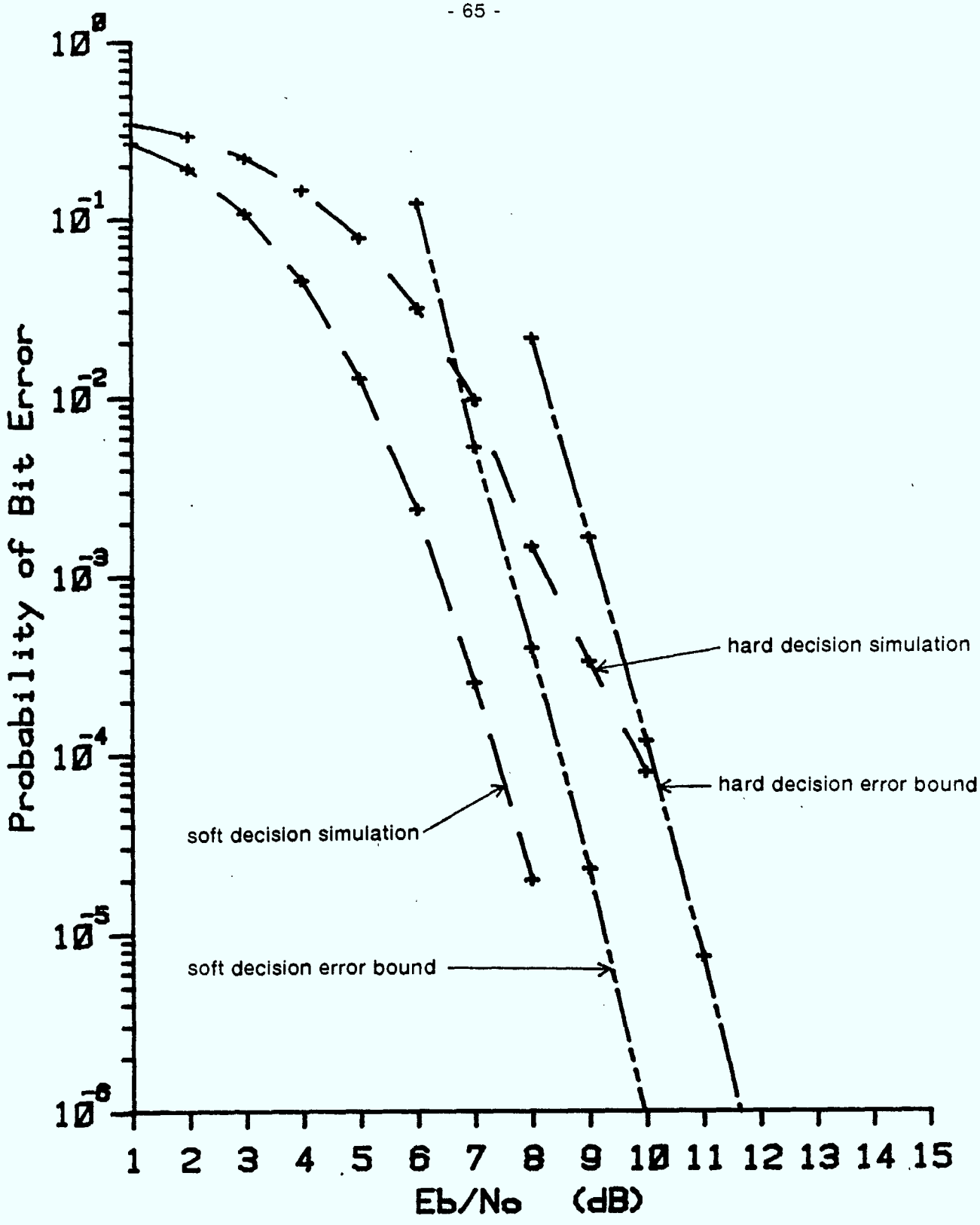

Figure 3.13 Case 2B Code Error Bounds (ν = 6), Coherent Reception

Rate = 2/4, 4 tones, Variable Signal Energy

The code used in this simulation case has a free distance of 6 which is approximately the same as the rate 2/3 codes in Case 2A. Therefore there is no appreciable performance gain for this system. The theoretical error bound for this code is shown in Figure 3.13.

3.2.5 Case 2C: Rate = 2/3, 4 tones, Constant Signal Energy

This simulation employs the same rate 2/3 convolutional codes as Case 2A. In this case, the eight signals required are constructed from four orthogonal tones. Single and double tone signals with constant signal energy are used. The codewords are mapped onto the signals to optimize the error performance as described in Chapter two.

The simulation results for coherent detection are plotted in Figure 3.14. The hard decision decoder performs worse than the baseline by 0.7 dB and 0.9 dB for the short and long constraint length codes respectively. Soft decisions give improved performance with a margin of 1.5 dB for the short constraint length code over the baseline. The longer code provides an additional gain of 0.5 dB for a 2.0 dB improvement on the reference system.

The noncoherent performance curves appear in Figure 3.15. The baseline system is again superior to hard decision decoding for both codes. The short constraint length code has a 0.4 dB disadvantage while the longer code has 0.3 dB worse performance. With soft decision decoding, the short constraint length coded system improves by 2.0 dB. The longer code shows 3.0 dB gain over the hard decision case for a 2.7 dB improvement over the reference system.

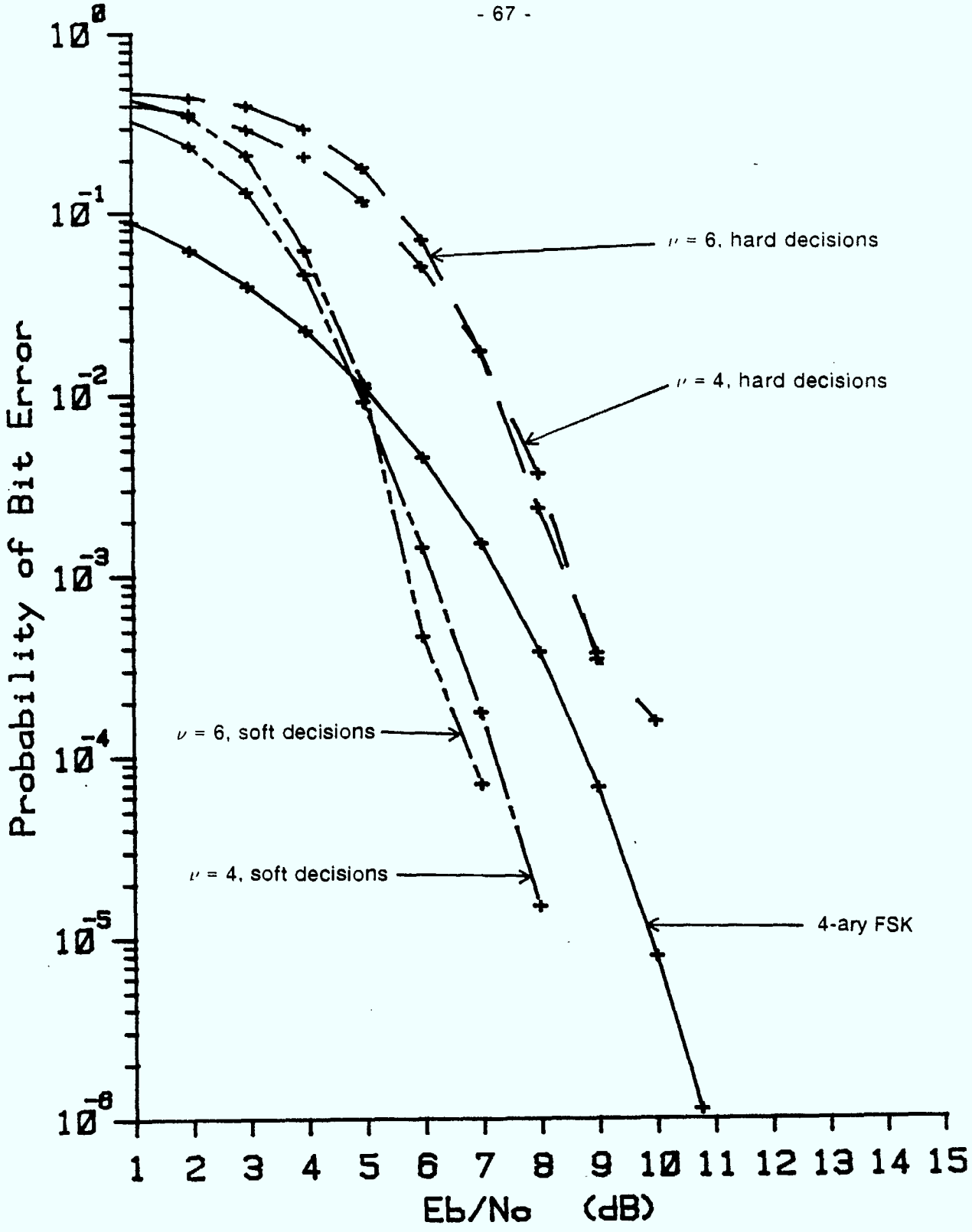

Figure 3.14 Case 2C Simulation Results, Coherent Reception

Rate = 2/3, 4 tones, Constant Signal Energy

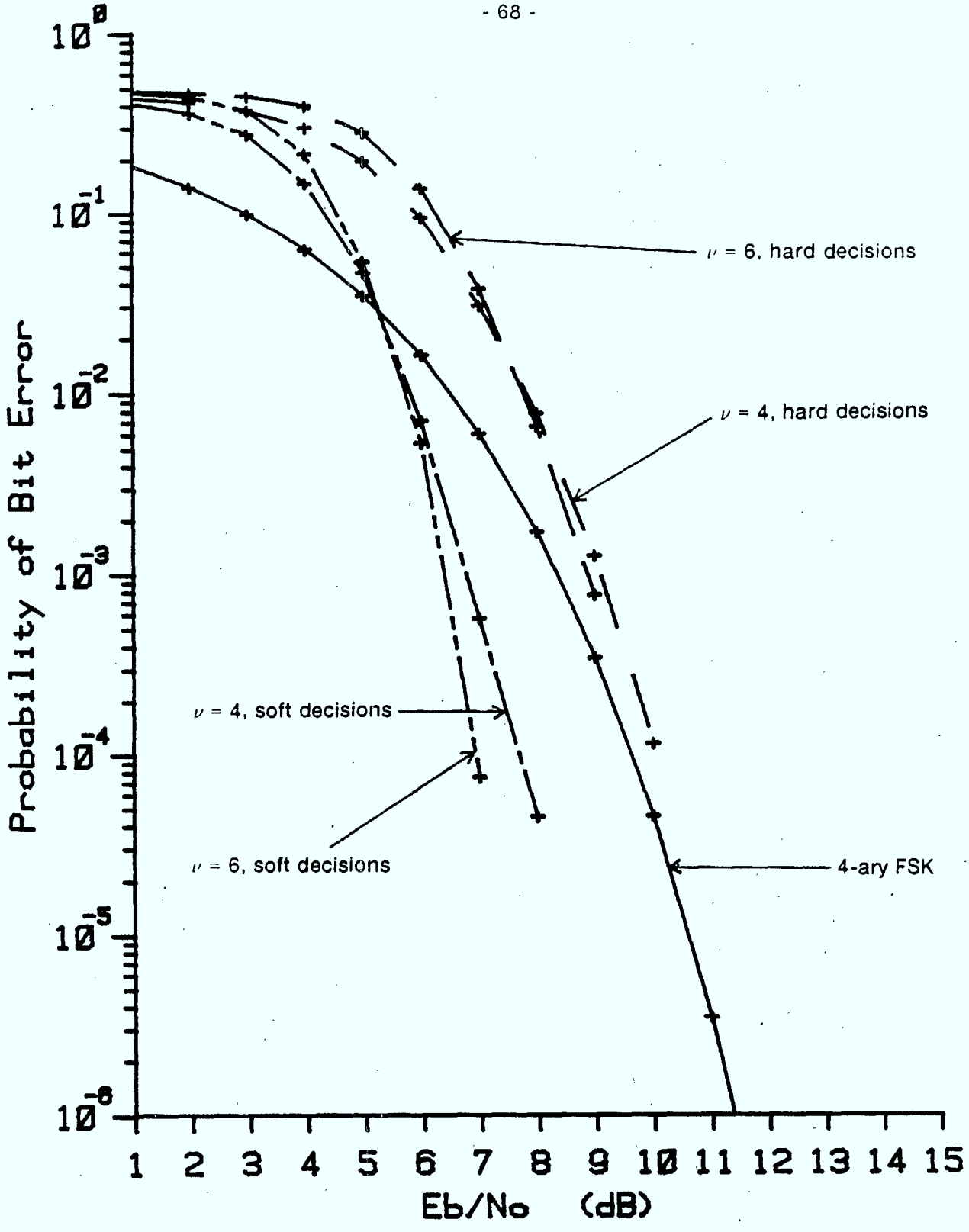

Figure 3.15 Case 2C Simulation Results, Noncoherent Reception

Rate = 2/3, 4 tones, Constant Signal Energy

This case has the best performance of the three simulations at this information rate. The additional advantage of constant energy signals imposes less stringent requirements on the actual transmitter and receiver.

3.2.6 Case 3A: Rate = 3/4, 4 tones, Variable Signal Energy

The final two cases have an information rate of three bits per signalling interval, which corresponds to a baseline system of 8-ary FSK. Case 3A employs a rate 3/4 code and a signal space of sixteen points. The signals are comprised of all possible combinations of four orthogonal tones, which require only one half the bandwidth of the baseline system. The simulation was run with one code which has a constraint length of 5 and a free distance of 5.

Figure 3.16 shows the results of the simulation for coherent reception. With hard decisions, the coded system is 1.9 dB worse than the baseline. Soft decisions yield a 2.1 dB improvement, resulting in a 0.2 dB advantage over FSK signalling. The performance of the noncoherent receiver appears in Figure 3.17. The hard decoder exceeds the reference system performance by 1.4 dB while soft decisions provide a 1.9 dB gain. This results in a modest 0.5 dB improvement over the baseline for the coded system with soft decision decoding.

This case does not provide significant performance gain over 8-ary FSK. The relatively high rate code provides a free distance of 5 and the signalling bandwidth is reduced by one half from the reference system. Figure 3.18 shows the error performance bounds for this code with a rectangular signal constellation. The signals also have variable energy, requiring increased receiver complexity.

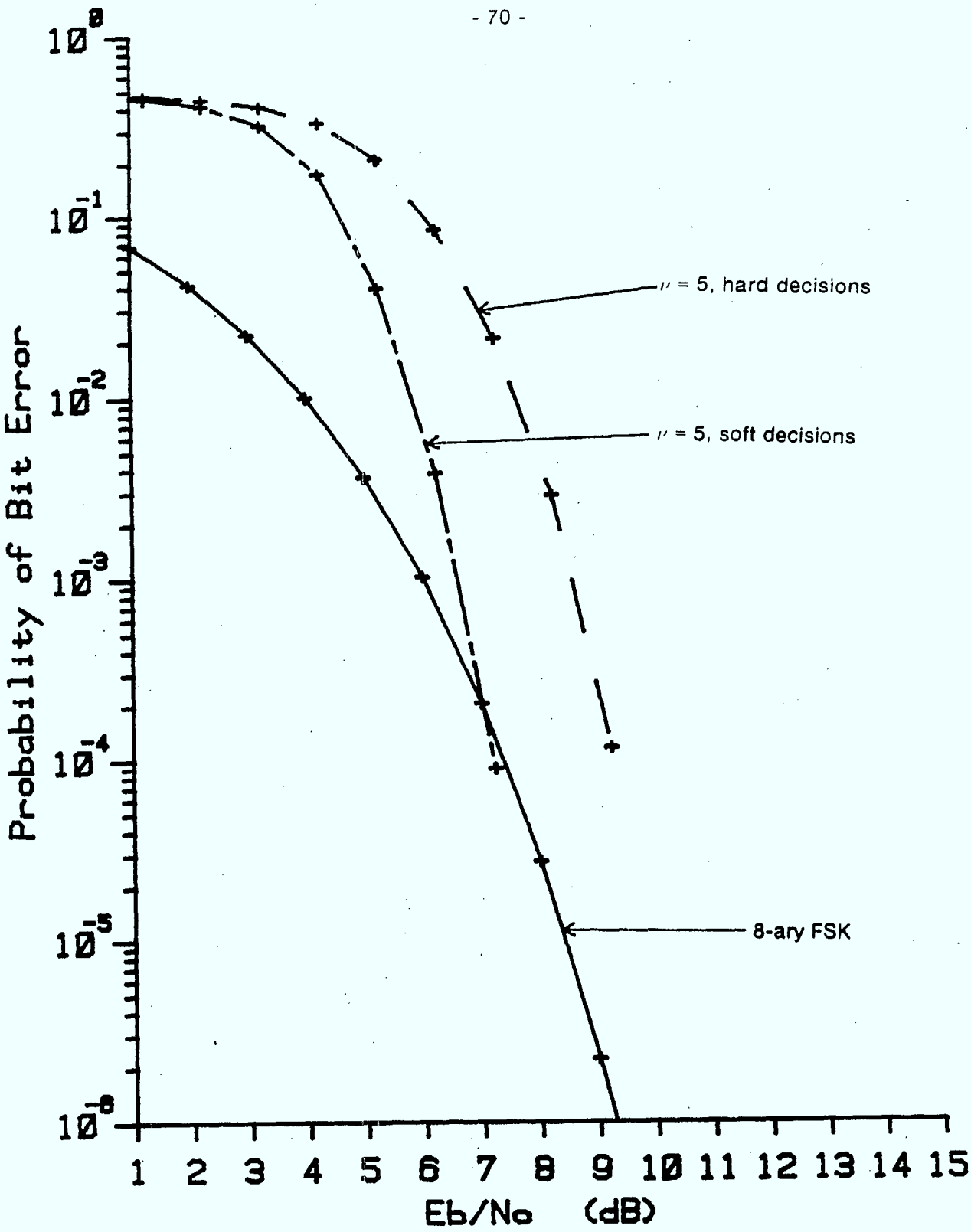

Figure 3.16 Case 3A Simulation Results, Coherent Reception

Rate = 3/4, 4 tones, Variable Signal Energy

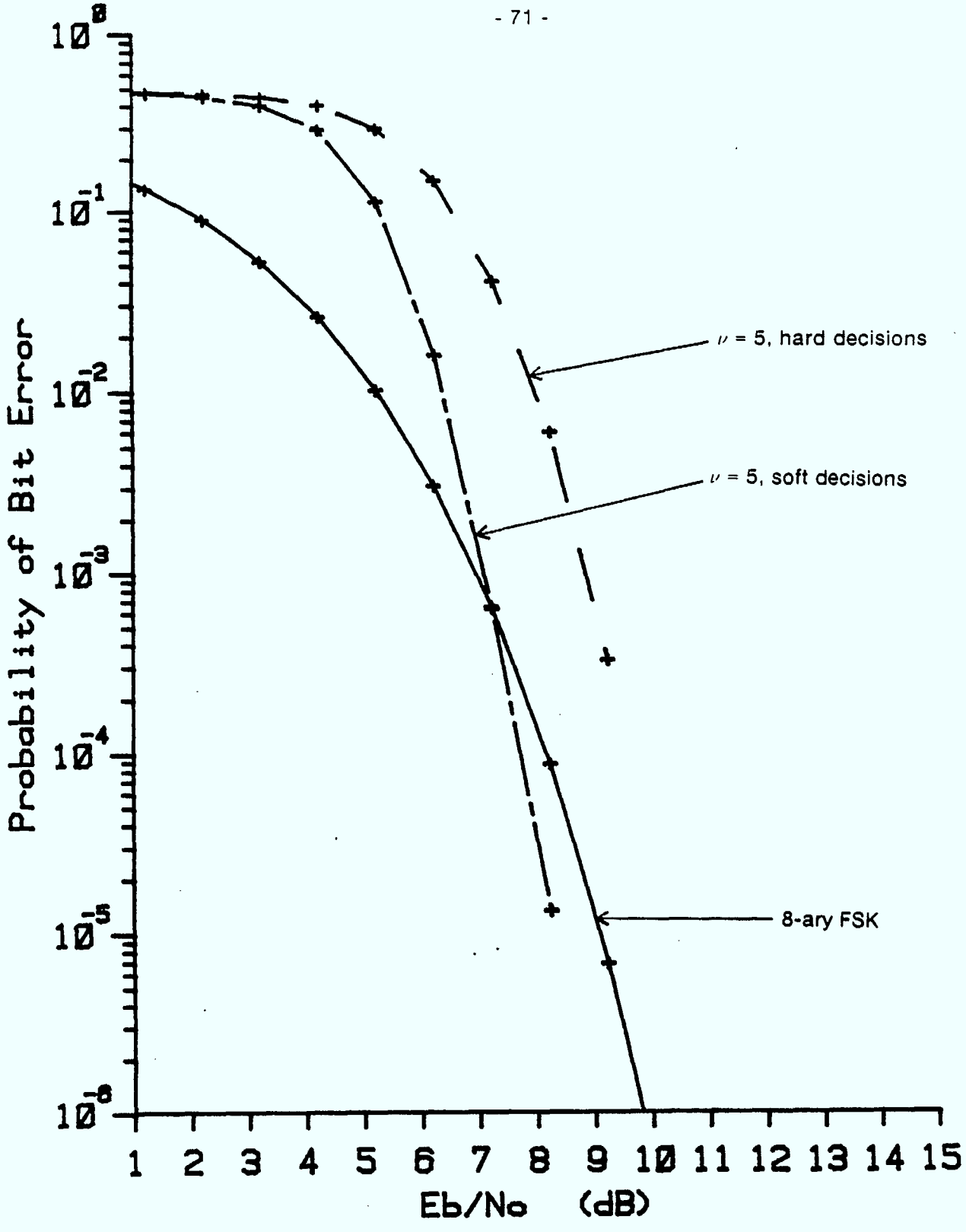

Figure 3.17 Case 3A Simulation Results, Noncoherent Reception

Rate = 3/4, 4 tones, Variable Signal Energy

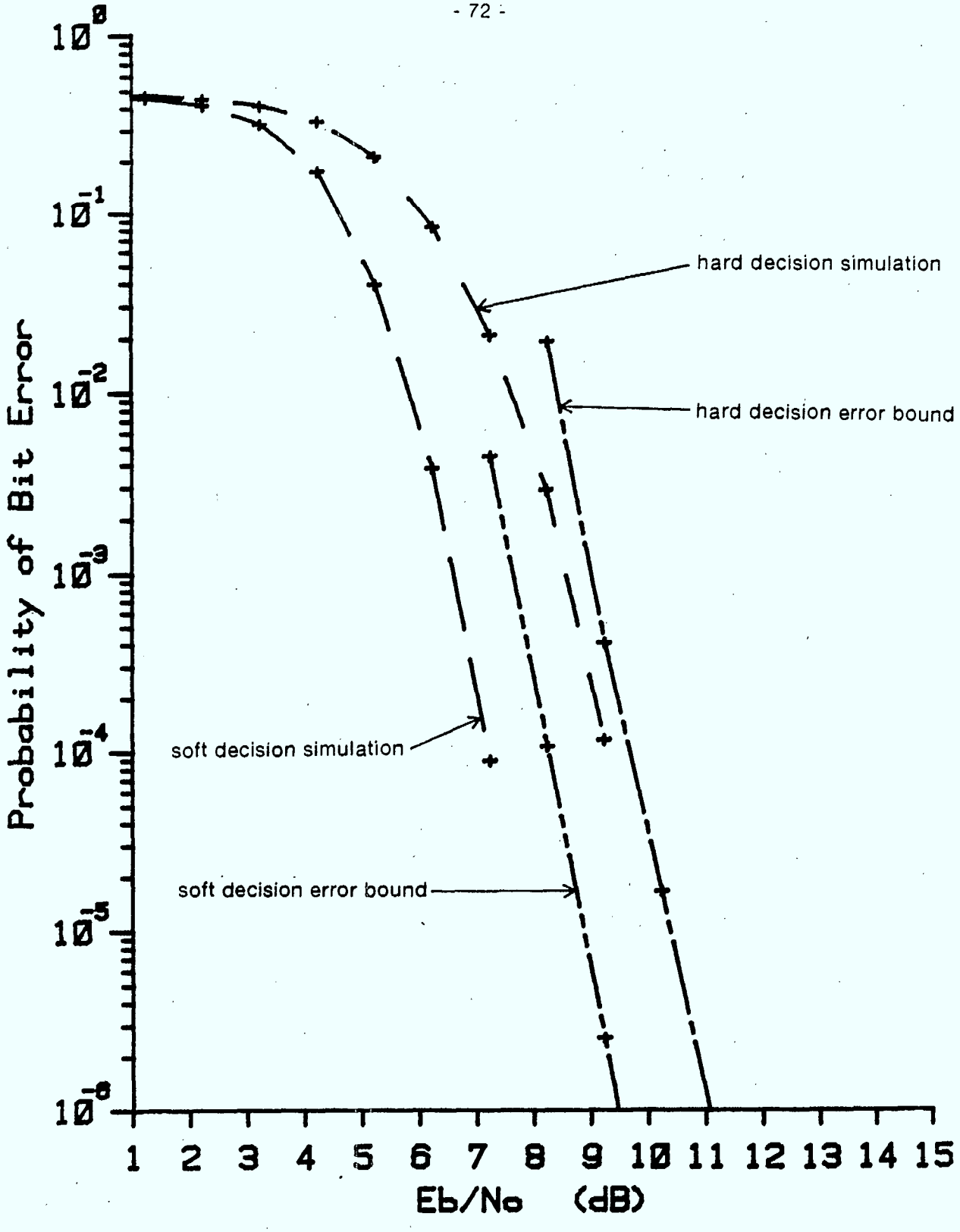

Figure 3.18 Case 3A Code Error Bounds ($\nu = 5$), Coherent Reception

Rate = 3/4, 4 tones, Variable Signal Energy

3.2.7 *Case 3B: Rate = 3/6, 8 tones, Constant Signal Energy*

The codes for this case have a rate of 3/6 and constraint lengths of 3 and 6. The short code is a dual-3 rate 1/2 convolutional code, and the longer code is comprised of three identical cascaded rate 1/2 encoders, each with $\nu = 2$. The sixty-four signals required are composed of single tones and triples of tones selected from a set of eight orthogonal tones. The signals have constant energy and are assigned to the codewords as previously described.

The performance curves for coherent reception are shown in Figure 3.19. The coded simulations with hard decision decoding are significantly worse than the baseline system. The margins are 4.3 dB for the short code and 2.5 dB for the longer code. The performance gains for soft decision decoding are also quite large so that the short constraint length code is 0.3 dB worse than the baseline with soft decison decoding. A gain of 2.4 dB over the reference system is achieved by the long code when soft decoder metrics are employed.

The results for noncoherent reception are quite similar to the coherent case as shown in Figure 3.20. The short code with hard decisions is 3.8 dB worse than the baseline, while the long code has a 1.8 dB disadvantage. The use of soft decision decoding provides the short code with a 0.4 dB improvement on the baseline performance. The long code outperforms the baseline by 2.4 dB with soft decisions.

The long constraint length code with soft decision decoding gives good performance in this case. The relatively poor results of the other simulations are due mainly to two factors. The structure of the shorter code is such that the codewords cannot be mapped onto the signal set to provide maximum distance between error paths.

This accounts for the large disparity between the different constraint length codes. The codes used do not have large free distances, and the signal space mapping does not provide proportionality between Hamming distance and Euclidean distance. Therefore the hard decision decoding metric has a large disadvantage compared to the soft decision case.

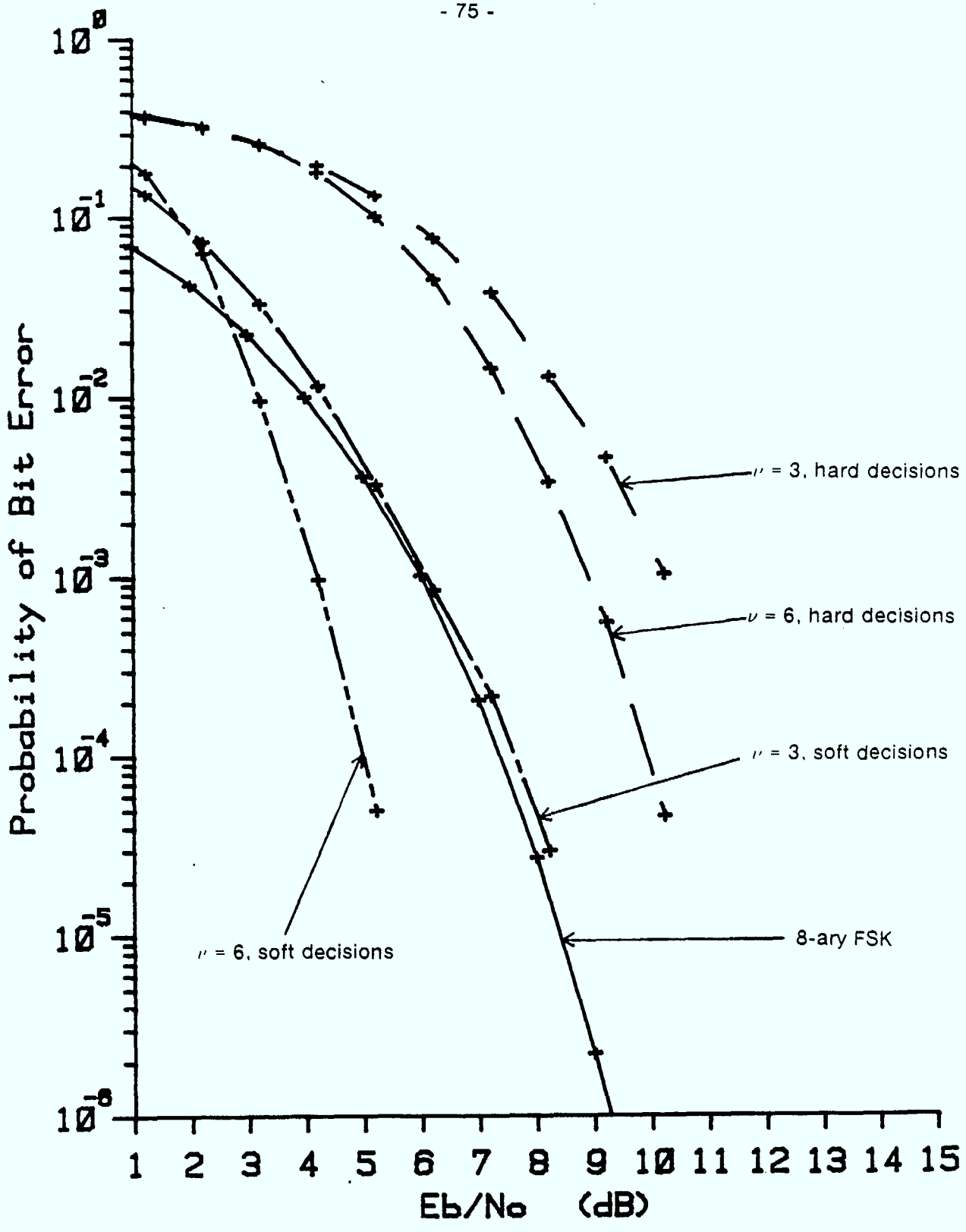

Figure 3.19 Case 3B Simulation Results, Coherent Reception

Rate = 3/6, 8 tones, Constant Signal Energy

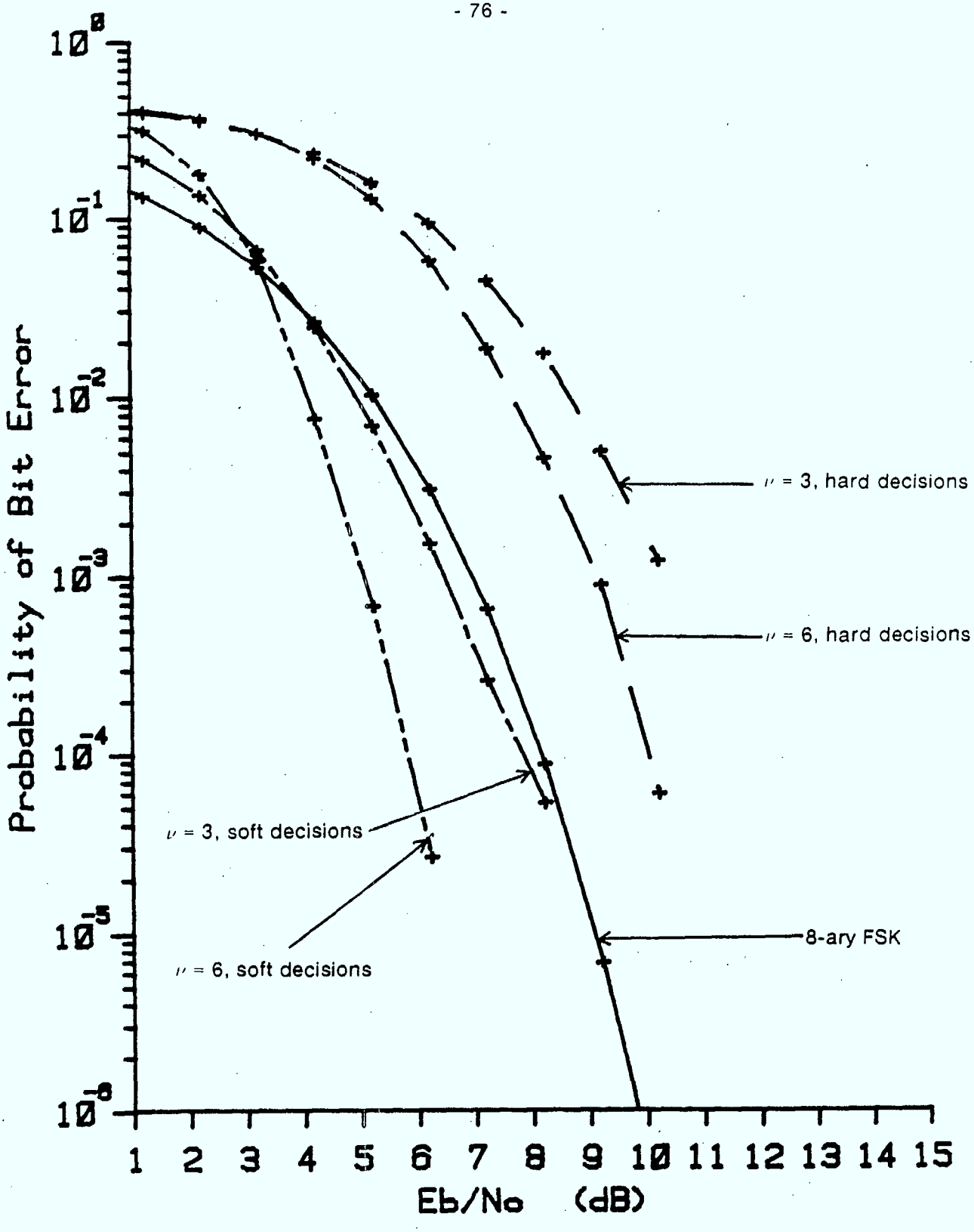

Figure 3.20 Case 3B Simulation Results, Noncoherent Reception

Rate = 3/6, 8 tones, Constant Signal Energy

CHAPTER FOUR

CONCLUSIONS

4.1 Findings of the Study

The major result of this study is quite obvious from the performance curves in the previous chapter. The use of convolutional coding with multiple tone signal sets gives significant improvement over FSK when soft decision decoding is employed. This performance gain is on the order of 2.0 dB (E_b/N_0) at a BER of 10^{-4} for at least one case at each information rate. There are numerous parameters of both the coding and modulation schemes which influence the results of the simulations.

The most readily apparent effect is caused by the type of decoding metric employed. The simulations with soft decision metrics indicate performance superior to those with hard decisions by a margin of from 1.5 to 4.9 dB. This situation would be expected because some information about the received signal is lost when a hard decision is made in the receiver. The difference is greater for schemes which have less correspondence between the Hamming distance of the codewords and the Euclidean distance between the signals, namely the constant signal energy constellations.

The performance of the coherent and noncoherent systems is very similar. In absolute terms, the coherent receiver gives superior performance due to the exact knowledge of the phase of the transmitted signal. However, the relative improvements for the coded systems and the gains for soft decision decoding are virtually identical for both types of receivers. Although noncoherent FSK is usually used in actual systems,

coherent results were presented for completeness. Also, theoretical error performance bounds can be calculated for coherent reception, and they provide verification of the simulation results.

The difference between the constant signal energy constellations and those with variable energy signals is difficult to accurately derive from the cases under consideration. The variable energy case proves superior for the transmission of a single bit per signalling interval. Case 1A shows the largest gains of all simulations, with gains of up to 5.1 dB. However, the use of constant energy signals with two tones involves a rather drastic reduction in signal spacing. The number of signals is also reduced significantly, and requires that a higher rate code be employed. These factors combine to cause the relatively poorer performance of Case 1B. The transmission of two bits per period provides the best opportunity for comparison of the constellations. The codes and the size of the signal sets are fairly similar in Cases 2A, 2B, and 2C. Under these conditions, neither of the two types of constellations appears significantly superior. The performance results for each simulation are within one dB for all three cases. When three bits are transmitted per signalling interval, the constant signal energy situation provides the best performance. However, Case 3A has a higher rate code and uses only one half the number of tones as in Case 3B. In spite of this, it actually has better performance for hard decision decoding, due to the signal space mapping.

There is another difference between constant and variable energy signal constellations that has more significance when considering actual implementation of the system. With variable energy signals, the transmitter output power varies according to the number of tones to be sent. A high peak to average power requirement might prove to be a disadvantage since the transmitter will be operating at less than its full peak

power capability for a large percentage of the time. The zero energy signal might also prove undesirable to implement if channel fading or drop-outs were possible. The receiver for unequal energy signals has increased complexity because of the necessity to compute an exponential function and a modified Bessel function in order to calculate each decision variable. However, the mapping of codewords onto the signal set is straightforward for this situation. In the constant signal energy case, the signal generator in the transmitter must adjust the amplitude of the signal tones to ensure the signal energy remains constant. The computation of decision variables in the receiver is simplified, but the mapping of codewords onto the signal space must be incorporated in both the transmitter and receiver.

4.2 Suggestions for Further Work

The results of this study raise some questions that may provoke further research. Although significant performance improvements have been discovered, further improvements may be obtained from different codes and signal constellations. One example of this might be codes with better distance profiles than the cascaded rate 1/2 codes used in this study, to improve hard decision performance. The use of larger signal spaces with lower rate codes is possible for eight tone and even sixteen tone signalling. Only 64 of 256 possible tone combinations were used in the signal set of Case 3B, and 16 tones provide 65,536 possible signals from which to construct a constellation. It is noteworthy that trellis coding in coherent communications systems obtains larger coding gains with larger signal sets [8]. Excessive computing time requirements for the simulation program used in this study precluded further exploration of larger signal sets.

Another subject for further investigation is the performance of these schemes in an anti-jamming system in the presence of jammer interference. Other studies [3, 4] have shown good results for convolutional coding with conventional FSK signalling, and so this is a promising area. The implementation of soft decision decoding becomes more complex in a jamming environment. Side information regarding the presence of a jamming signal is required by the decoder or else soft decision decoding seriously degrades in performance.

4.3 Summary

The use of convolutional codes with multiple tone signals has been shown to provide performance improvements over M-ary FSK signalling. The coded system does not require additional bandwidth to maintain the same information rate. Indeed in some cases a smaller modulation bandwidth and hence higher processing gain appears possible. The coding is suitable for implementation in a frequency hopped spead spectrum anti-jam system with a usual spectrum analyzing receiver followed by a Viterbi decoder. Increased performance gains through different codes and signal sets, as well as performance in a jamming environment are topics of further interest.

REFERENCES

1. Stark, Wayne E., "Coding for Frequency Hopped Spread Spectrum Communication with Partial Band Interference", **IEEE Transactions on Communications**, Vol. COM-33, No. 10 (Oct. 1985), pp. 1036-1057.

2. Pursley, Michael B. and Stark, Wayne E., "Performance of Reed-Solomon Coded Frequency Hopped Spread Spectrum Communications in Partial Band Interference", **IEEE Transactions on Communications**, Vol. COM-33, No. 8 (Aug. 1985), pp. 767-774.

3. Ma, Howard H. and Poole, Margaret A., "Error-Correcting Codes Against the Worst-Case Partial-Band Jammer", **IEEE Transactions on Communications**, Vol. COM-32, No. 2 (Feb. 1984), pp. 124-133.

4. Torrieri, Don J., "Frequency Hopping with Multiple Frequency Shift Keying and Hard Decisions", **IEEE Transactions on Communications**, Vol. COM-32, No. 5 (May 1984), pp. 574-582.

5. Pawula, R. F. and Golden, R., "Simulations of Convolutional Coding/Viterbi Decoding with Noncoherent CPFSK", **IEEE Transactions on Commmunications**, Vol. COM-29, No. 10 (Oct. 1981), pp. 1522-1526.

6. Keightley, R. J., "A Simulation of Frequency-Dehopped Binary and 4-ary NC-FSK Signals", Communications Research Centre, Ottawa, Canada, Technical Note No. 722, April 1984.

7. Ungerboeck, Gottfried, "Channel Coding with Multilevel/Phase Signals", **IEEE Transactions on Information Theory**, Vol. IT-28, No. 1 (Jan. 1982), pp. 55-66.

8. Ungerboeck, Gottfried, "Trellis-Coded Modulation with Redundant Signal Sets", **IEEE Communications Magazine**, Vol. 25, No. 2 (Feb. 1987), pp. 5-21.

9. Calderbank, A. Robert and Mazo, James E., "A New Description of Trellis Codes", **IEEE Transactions on Information Theory**, Vol. IT-30, No. 6 (Nov. 1984), pp. 784-791.

10. Thapar, Hemant K., "Real-Time Application of Trellis Coding to High-Speed Voiceband Data Transmission", **IEEE Transactions on Selected Areas in Communications**, Vol. SAC-2, No. 5. (Sept. 1984), pp. 648-658.

11. Wozencraft, John M. and Jacobs, Irwin Mark, **Principles of Communication Engineering**, John Wiley and Sons Inc., 1965.

12. Viterbi, Andrew J. and Omura, Jim K., **Principles of Digital Communication and Coding**, McGraw-Hill Book Co., 1979.

13. Golomb, S. W. (editor), **Digital Comunications with Space Applications**, Prentice-Hall Inc., 1964.

14. Clark, George C. and Cain, J. Bibb, **Error Correction Coding for Digital Communications**, Plenum Press, 1981.

15. Larsen, Knud J., "Short Convolutional Codes with Maximal Free Distance for Rates 1/2, 1/3, and 1/4", **IEEE Transactions on Information Theory**, Vol. IT-19, No. 3 (May 1973), pp. 371-372.

16. Paaske, Erik, "Short Binary Convolutional Codes with Maximal Free Distance for Rates 2/3 and 3/4", **IEEE Transactions on Information Theory**, Vol. IT-20, No. 5 (Sept. 1974), pp. 683-689.

17. Odenwalder, J. P., **Dual-k Convolutional Codes for Noncoherently Demodulated Channels**, Proc. IEEE Int. Telem. Conf., 1976.

18. Forney, G. David, "The Viterbi Algorithm", **Proceedings of the IEEE**, Vol. 61, No. 3 (March 1973), pp. 268-278.

19. Heller, Jerrold A. and Jacobs, Irwin Mark, "Viterbi Decoding for Satellite and Space Communication", **IEEE Transactions on Communications Technology**, Vol. COM-19, No. 5 (Oct. 1971), pp. 835-848.

20. Viterbi, Andrew J., "Orthogonal Tree Codes for Comunication in the Presence of White Gaussian Noise", **IEEE Transactions on Communications Technology**, Vol. COM-15, No. 2 (April 1967), pp. 238-242.

21. Simon, Marvin K., Omura, Jim K., Scholtz, Robert A., and Levitt, Barry K., **Spread Spectrum Communications, Volume I**, Computer Science Press Inc., 1985.

22. Omura, Jim K. and Levitt, Barry K., "Coded Error Probability Evaluation for Antijam Communication Systems", **IEEE Transactions on Communications**, Vol. COM-30, No. 5 (May 1982), pp. 896-903.